

Dynamics of preventive versus post-diagnostic cancer control using low-impact measures

Andrei R. Akhmetzhanov^{1,2} and Michael E. Hochberg^{1,3,4,}*

¹ *Institute of Evolutionary Sciences of Montpellier - UMR 5554, University of Montpellier II, CC065, Place Eugène Bataillon, 34095 Montpellier Cedex 5, France*

² *Theoretical Biology Lab, Department of Biology, McMaster University, Hamilton, Ontario L8S4K1, Canada*

³ *Santa Fe Institute, Santa Fe, NM 87501, USA*

⁴ *Wissenschaftskolleg zu Berlin, Wallotst. 19, 14193 Berlin, Germany*

^{*} *To whom correspondence should be addressed. E-mail: mhochber@univ-montp2.fr*

Abstract

Cancer poses danger because of its unregulated growth, development of resistant subclones, and metastatic spread to vital organs. We currently lack quantitative theory for how preventive measures and post-diagnostic interventions are predicted to affect risks of a life threatening cancer. We evaluate how continuous measures such as life style changes and traditional treatments affect both neoplastic growth and the frequency of resistant clones. We then compare and contrast preventive and post-diagnostic interventions assuming that only a single lesion progresses to invasive carcinoma during the life of an individual, and resection either leaves residual cells, or metastases are undetected. Whereas prevention generally results in more positive therapeutic outcomes than post-diagnostic interventions, this advantage is substantially lowered should prevention initially fail to arrest tumour growth. We discuss these results and other important mitigating factors that need to be taken into consideration in a comparative understanding of preventive and post-diagnostic interventions.

Keywords: evolution of resistance, chemoprevention, tumour management, resection, post-diagnostic intervention, drug addiction, maximum tolerated dose, metronome therapy

Introduction

Mathematical models play an important role in describing and analysing the complex process of carcinogenesis. Natural selection for increases in tumour cell population growth can be represented as the net effect of increased cell division rates and/or decreased apoptosis (*e.g.*, (1)). Relatively rare driver mutations confer such a net growth advantage, whereas numerically dominant passenger mutations with initially neutral or mildly deleterious effects (2,3,4) can increase in frequency due to genetic hitchhiking or subsequent positive selection. Amongst the many passengers in a growing tumour, some can contribute to chemoresistance, and sufficiently large tumours could contain different clones that, taken as a group, can resist some, if not most, possible chemotherapies (see (5) for resistance to imatinib). Chemotherapeutic remission followed by relapse suggests that these resistant cells are often present at low frequencies prior to therapy, either due to genetic drift or costs associated with resistance. Resistant phenotypes subsequently increase in frequency during radiotherapy or chemotherapy, and through competitive release, they may incorporate one or more additional drivers, resulting in accelerated growth compared to the original tumour (6).

Previous mathematical studies have considered alternatives to attempting to minimize or eradicate clinically diagnosed cancers with maximum tolerated doses (MTD) of chemotherapeutic drugs. This body of work indicates that MTD is particularly prone to select for chemoresistance (*e.g.*, (7,8,9)), and what little empirical work exists supports this basic prediction (10), but see (11) for other disease systems). Numerous alternatives to the goal of cancer minimization/eradication have been investigated (*e.g.*, (2,7,12,13,14)). For example, Komarova and Wodarz (12) considered how the use of one or multiple drugs could prevent the emergence or curb the growth of chemoresistance. They showed that the evolutionary rate and associated emergence of a diversity of chemoresistant lineages is a major determinant in the success or failure of multiple drugs versus a single one. Lorz and co-workers (9) recently modelled the employment of cytotoxic and cytostatic therapies alone or in combination and showed how combination strategies could be designed to be superior in terms of tumour eradication and managing resistance than either agent used alone. Foo and Michor (7) evaluated how different dosing schedules of a single drug could be used to slow the emergence of resistance given toxicity constraints. One of their main conclusions is that drugs slowing the generation of chemoresistant mutants and subsequent evolution are more likely to be successful than those only increasing cell death rates.

These and other computational approaches have yet to consider the use of preventive measures to reduce cancer-associated morbidity and mortality, whilst limiting resistance. Prevention includes life-style changes and interventions or therapies in the absence of detectable invasive carcinoma (*e.g.*, (15,16,17,18)), for example reduced cigarette consumption (19) or chemoprevention (20). In depth consideration of preventive measures and their likely impact on individual risk and epidemiological trends is important given the likelihood that all individuals harbour pre-cancerous lesions, some of which may transform into invasive carcinoma (21,22), and concerns

as to whether technological advances will continue to make significant headway in treating clinically detected cancers (23,24).

Here we model how continuous, constant measures affect tumour progression and the emergence of resistant lineages. We assume that an individual can contract at most a single cancer, originating from a single lesion. Importantly, we consider cases where the measure may select for the evolution of resistant phenotypes and cases where no resistance is possible. Our approach is to quantify the daily extent to which a growing neoplasm must be arrested in order to either eradicate it or to delay a potentially lethal cancer. Several authors have previously argued how constant or intermittent low toxicity therapies either before or after tumour discovery could be an alternative to maximum tolerated dose chemotherapies (18,25), but to our knowledge no study has actually used quantified the extent to which cancer cell population growth needs to be arrested for such approaches to succeed (2,26,27). Below we employ the terms ‘treatment’, ‘measure’, and ‘therapy’ interchangeably, all indicating intentional measures to arrest cancer cell population growth.

We first derive analytical expressions for the expected total number of cells within a tumour at any given time. We explore dynamics of tumour sizes at given times, and times to detection for given tumour sizes. Specifically, we show that the expected mean tumour size in a population of subjects can be substantially different from the median, since the former is highly influenced by outliers due to tumours of extremely large size. We then consider constant daily preventive measures, and show that treatment outcome is sensitive to initial conditions, particularly for intermediate sized tumours. Importantly, we provide approximate conditions for tumour control both analytically and numerically using empirical parameter estimates. We next consider post-diagnostic interventions in which tumour resection either is not complete and leaves residual cells, or undetected metastases are present. We contrast these with prevention scenarios where (1) there is no difference in the age at which either prevention or post-diagnostic intervention commences, and (2) prevention and post-diagnostic interventions are alternatives, i.e., the former always occurs before the latter. We show as expected that therapeutic outcomes are generally superior under prevention versus post-diagnostic intervention, and that higher impacts on the cancer cell population are usually required for post-diagnostic interventions to achieve a level of control comparable to prevention. Moreover, we find that should post-diagnostic resection leave sufficiently large numbers of residual cells (or metastases are not discovered), then a range of the most successful outcomes under prevention are not attainable under post-diagnostic intervention regardless of potential cell arrest. Finally and importantly, whereas there is little gained in terms of outcomes in post-diagnostic intervention beyond c 0.3% cell arrest per day for both small (10,000) and large (1 million) cancer cell populations, prevention outcomes may achieve continual gains up to c 0.6% for the latter cell number.

Modelling framework

Previous study has evaluated the effects of deterministic and stochastic processes on tumour growth and the acquisition of chemoresistance ((12,27,28), see review (29)). We first consider both processes through exact solutions and numerical simulations of master equations, using the mean field approach. A mean field approach assumes a large initial number of cells (30) and averages any effects of stochasticity, so that an intermediate state of the system is described by a set of ordinary differential equations (*i.e.*, master equations; (31)). Solutions to these are complex even in the absence of the explicit consideration of both drivers and passengers (32,33).

We do not explicitly model different pre-cancerous or invasive carcinoma states. Rather, our approach follows the dynamics of the relative frequencies of subclones, each composed of identical cells (34,35). We simulate tumour growth using a discrete time branching process for cell division (27,36,37). For each numerical experiment, we initiate a tumour of a given size and proportion of cells resistant to the measure under consideration within a tumour.

Briefly, the model framework is as follows. Each cell in a population is described by two characteristics. The first is its resistance status to the measure, which is either “not resistant” ($j = 0$) or “resistant” ($j = 1$). The second property is the number of accumulated driver mutations (maximum N) in a given cell line. At each time step of 4 days cells either divide or die, and when a cell divides, its daughter cell has a probability u of producing a driver mutation and v of producing a resistant mutation. We assume no back mutation and that cells do not compete for space or limiting resources (see Discussion).

The fitness function f_{ij} , the difference between the birth and death rates of a cell, is defined by the number of accumulated drivers ($i = 0, 1, \dots, N$) and resistance status ($j = 0, 1$): a sensitive cancerous cell with a single driver has selective advantage s , and any accumulated driver adds s to fitness, while resistance is associated with a constant cost c . Exposure to a single treatment affects only non-resistant cells ($j = 0$), incurring a loss σ to their fitness. Thus, the fitness function is:

$$f_{ij} = s(i + 1) - \sigma(1 - j) - cj.$$

The assumption of driver additivity is a special case of multiplicative fitness, and both are approximately equivalent for very small s .

We conducted numerical experiments each with the same initial states, but each using a unique set of randomly generated numbers of a branching process. For each simulation and each time step, the number of cells at time $(t + 1)$ was sampled from a multinomial distribution of cells at time t (see (27,36) for details). Table 1 presents baseline parameter values employed in this study. Hereafter, we refer to σ as the treatment intensity (applied once every cell cycle of 4 days), while the corresponding daily arrest level to non-resistant cells is $\sigma/4$.

Results

Preventive measures

We first studied preventive interventions where a patient has a high risk of developing a cancer and/or a biomarker indicates the probable presence of a cancer. In either case, so that we can compare and contrast different intervention levels, we assume that the (undetected) tumour actually contains M_0 cells when prevention commences. We examine effects on the mean by considering the distribution of tumour sizes at different times using mean-field dynamics (see Appendix 1). Numerical experiments were then conducted by assuming that initially tumours contained $M_0 = 10^6$ identical cells ($i = 0$), of which 0.01% were resistant. These assumptions are obviously oversimplifications, and we relax some of them below and in the next section.

There is an excellent correspondence between analytical and numerical results for σ varied in range of s (Appendix 1 – figure 1). A more detailed study of the distribution of tumour sizes reveals that the mean diverges considerably from median behaviour in the majority of cases, since the former is strongly influenced by outliers with high tumour cell numbers (see Appendix 1 – figures 1B and 2).

Figure 1 shows four examples of numerical experiments. An untreated tumour reaches the detection threshold of 10^9 cells by $c. 18$ years on average, and because it is not subject to strong negative selection (we assume low c), any emerging resistant cell-lines are likely to remain at low frequency (0.03% at the time to detection in the example of Figure 1A). In Figure 1B, low treatment intensity delays tumour growth and thus time of detection by $c. 16$ years, while an increase in dose tends to result in tumours dominated by resistant cells (Figure 1C). Despite being unaffected by treatment, resistant cell populations are sometimes observed to go extinct due to stochasticity (Figure 1D), and this tends to occur more at high treatment levels, because there are fewer sensitive tumour cells to seed new (mutant) resistant cell populations.

We next considered how therapies affected the distribution of tumour detection times in cases where cancer cell population attained the threshold of 10^9 cells. The magnitude of the selective advantage s shows that tumour growth is largely driven by its non-resistant part for relatively low impact treatments $\sigma < 2s$ (Figure 2). Importantly, the tumour shifts from being mainly non-resistant to resistant at $\sigma \approx 2s$, which is reflected by the inflection point in the trajectory of the median (indicated by point B in Figure 2). Notice that detection times are also most variable at $\sigma \approx 2s$. The median changes smoothly at high treatment levels ($\sigma > 2s$), tending to a horizontal asymptote. This is explained by the fact that the sensitive part is heavily suppressed at high treatment levels, meaning that the dynamics are strongly influenced by the actual time point at which the first resistance mutation occurs.

We find, counterintuitively, that early-detected tumours are more likely to be resistant under constant treatments than those detected at later times (A, B, C in Figure 2C). This is because tumours under treatment that by chance obtain resistance early grow faster than those that do not. We find that by the time of detection, non-resistant tumours usually accumulate up to 4 additional

drivers on average, while resistant tumours have fewer. For larger values of c , an additional non-regularity emerges (segment DEF in Figure 2B), appearing at $\sigma \approx 3s$ and is associated with tumours having a majority of cells with maximum numbers of drivers. This region is also characterized by a different transition to complete resistance (compare Video 1 for relatively low and high costs of resistance, respectively). For example, at point D , tumours with a majority of non-resistance have less variable detection times than tumours with a majority of resistant cells (B and corresponding panel C in Figure 2). Treatment levels along the segment DEF result in tumours that are more likely to be resistant as one goes from the centre to the tails of the distribution of detection times. This differs qualitatively from the previous case of low cost of resistance, where the tumours are less resistant in the tail of the distribution of detection times (Figure 2C).

The inflection point at $\sigma \approx 2s$ in Figure 2A is due to the accumulation of additional drivers within tumours and associated increases in the likelihood that the tumour eventually resists treatment. Since the initial population consists of 10^6 cells, in the absence of treatment, a mutant cell with one additional driver and associated fitness $2s$ will appear very rapidly. Such a tumour can be suppressed only if $\sigma > 2s$. This is supported by additional numerical experiments, where we vary the maximal number of additional driver mutations N : the inflection point $\sigma \approx 2s$ disappears when $N = 0$ (Figure 2 – figure supplement 1A). The inflection points at $\sigma = 3s, 4s$ emerge at treatment levels that effectively suppress sensitive subclones with the most drivers before resistance mutations are obtained (*cf* Figure 2 – figure supplement 1A,C-D with Figure 2 – figure supplement 1B and Video 1). Specifically, the peaked distributions, corresponding to better therapeutic outcomes, tend to disappear when resistant subclones emerge.

The initial cell number M_0 affects both the median and distribution of detection times (Figure 2 – figure supplement 1C). For large initial tumours, growth is deterministic and exponential. As the initial size is decreased from 10^6 to 10^5 , stochastic effects are increasingly manifested by greater variability in tumour inhibition and an inflection point observed at the 95th percentile. Moreover, we find that a tumour is likely to be eradicated under a range of constant treatments when $M_0 = 10^5$ or fewer initial cells; in contrast, a tumour is virtually certain to persist regardless of treatment level for $M_0 = 10^7$ cells or greater (Figure 2 – figure supplement 2A,B). In other words, our model indicates that tumours that are *c.* 1% the size of most clinically detectable, internal cancers will typically be impossible to eradicate with a single therapy.

Given the mutation rates assumed here, we can expect that many tumours with one million cells will either already contain or rapidly, subsequently acquire resistant cells (38). It is therefore not surprising that the initial fraction of resistant cells in a tumour has little impact on dynamics (Figure 2 – figure supplement 1D). In contrast, another measure of success in control (the fraction of persons with tumours that remain undetected after 50 years of growth) improves substantially with lower numbers of initial resistance mutations, particularly at higher treatment levels (Figure 2 – figure supplement 2C). This is because the initial phases of treatment have a major impact on the potential for new resistant mutants, and should few resistance mutations be initially present or emerge during the initial phases of treatment, they will either go stochastically extinct or will not

grow to detection levels (1 billion cells) in the 50 year time frame of these numerical experiments.

We conducted further sensitivity analyses by varying accumulation rates of additional driver mutations u . We find that tumours exhibit more or less deterministic growth depending on the relation between the initial number of cells M_0 and driver mutation rate u , which is analogous to the phenomenon shown in Figure 2 – figure supplement 1D, whereby the higher the mutation rate, the less apparent are stochastic effects. The corresponding analysis is presented in Section B of the Appendix 1 and Figure 5 therein.

Finally, we considered scenarios where costs of resistance were dose-dependent, and specifically situations of drug addiction (39). Numerical studies presented in more detail in Section C of the Appendix 1 show that under dose-dependent costs, a drug treatment only applied when the number of non-resistant cells exceeds the number of resistant cells (e.g., a metronomic therapy (40)) leads to slower long-term tumour growth than does a constant therapy.

Post-diagnostic interventions

We next investigated how a post-diagnostic measure (usually some form of chemotherapy or radiation therapy, but could also involve adjuvants after an initial therapy) affects the probability of treatment success, the distribution of times for tumour relapse and resistance levels. We assume that a tumour grows from one cell ($i = 0, j = 0$) and is discovered either at 10^9 (early) or 10^{11} (very late) cells, whereupon the primary tumour is removed, leaving a small number (10^4 or 10^6) of residual, and/or undetected or inoperable neighbouring micro-metastatic cells, and/or distant metastatic cells. Below, we contrast this with prevention without discriminating the age at which either prevention or post-diagnostic interventions commences, whereas in the following section we consider these approaches at competing alternatives. Figure 3A and Figure 3 – figure supplement 1A present the distributions of driver mutations for each scenario. (Recall that in the previous section we assumed that when a measure commenced, tumours had no additional drivers ($i = 0$) and 0.01% resistance).

First, we examine the case where post-diagnostic resection leaves 10^6 cells. As suggested by our studies above on prevention, one million cells have a high probability of already containing resistant subclones, and deterministic effects dominate subsequent tumour growth dynamics. Comparing the median expectations of years from tumour excision to relapse, early discovery (at 10^9 cells) yields an additional 3.4 years compared to late discovery (at 10^{11} cells) at $\sigma = 1.5\%$ (medians for low vs. high detection thresholds are 14.8 and 11.4 years, respectively; Figure 3B). Consider the following example: 20 years after resection and commencing treatment, the probability of tumour non-detection (i.e., the tumour is either eradicated or does not reach the detection threshold) is close to zero, regardless of treatment intensity (Figure 3D). Contrast this with cases of prevention starting at the same tumour size (10^6 cells), but which fail to control the incipient tumour for the 50 years of the simulation: the detection of these potentially life-

threatening tumours is substantially later than either of the excision cases (median 25.5 years for $\sigma = 1.5\%$, i.e., c 0.3-0.4% potential cell arrest per day), and tumours are managed below the detection threshold after 20 years in more than 80% of cases for any $\sigma > 1.0\%$ (Figure 3D).

Now consider a residual population of $1/100^{\text{th}}$ the previous case, that is 10^4 cells. Here, stochastic effects play a more important role in dynamics (Figure 3 – figure supplement 1). Due to initial heterogeneity (i.e., the co-occurrence of many subclones), when there are 4 and 5 (5 and 6) additional drivers in the dominant subclones of a residual cancer from an excised tumour of 10^9 (10^{11}) cells, we observe a double peak at, respectively, 4s and 5s (5s and 6s) (cf. Figure 3 – figure supplement 1B). These peaks in variability of outcomes are a result of the stochastic nature of the appearance of the first resistance mutations and of additional driver mutations. Interestingly, the secondary detection times (i.e., when residual or metastatic cells grow to form a new tumour) are more variable for small initial tumours compared to larger ones (cf. the median 35.8 years, 90% CIs [17.0, 70.5] years vs. 22.4, [13.7, 37.0] years for 10^9 vs. 10^{11} , respectively, with $\sigma = 1.5\%$). This effect is due to resistance emergence in more aggressive subclones for larger tumours, such that the tumour relapses more deterministically (i.e., with less variability, and faster on average). The distribution of the mean number of accumulated drivers within tumours and the probability of tumour non-detection after 20 years are shown in Figure 3 – figure supplement 1C and 1D, respectively.

Importantly, for both thresholds of tumour excision, subsequent cancer cell arrest levels beyond approximately $\sigma = 1.5\%$ make little difference in terms of tumour growth (Figure 3D), since virtually all of the sensitive cells post-excision will be arrested or killed by the measure beyond this level, leaving uncontrollable resistant cells to grow and repopulate the primary tumour site and/or metastases. (Note that this level is above that found in the previous section. This is because drivers accumulated throughout tumour growth in the results given in Figure 3, whereas they were assumed to only start accumulating the first drivers after growth from M_0 cells in Figures 2 and 3). Moreover, we find that for post-diagnostic interventions, data on time to clinical discovery (a proxy for age at discovery) and driver number are less predictive of therapeutic outcome as treatment intensity increases (Figure 3 – figure supplement 2-5). In particular, knowledge about the number of drivers at the time of tumour discovery is a better predictor of outcome than information about the time from tumour initiation to discovery (cf. Figure 3 – figure supplement 2,3 and 4,5).

Prevention vs. post-diagnostic intervention

The above results consider preventive measures and post-diagnostic interventions as independent rather than alternative approaches. Thus, although prevention delays tumour growth for longer times on average than does post-diagnostic intervention, because prevention is *always* initiated before diagnosis, when considering the relative benefits and risks of prevention versus eventual post-diagnostic intervention, the actual time gained by the former in terms of cancer-free life will be less than the differences reported in Figure 3B and Figure 3 – figure supplement 1B.

Figure 4 presents a hypothetical comparative scenario of prevention versus post-diagnostic intervention. Prevention may either succeed without recurrence, or should the measure initially fail and a tumour be clinically detected, the patient has a ‘second chance’, whereby the tumour is resected and treatment continued (assumed at the same treatment intensity σ), either to a further relapse (failure) or non-detection (success) (Figure 4A). Compare this scenario with the more standard post-diagnostic resection followed by treatment, which either results in relapse, or detection-free life (Figure 4B). These numerical experiments assume the same starting point (time at which the cancer cell population equals M_0 , and drivers and resistant subclones are present) for each tumour, and because of the addition a ‘second chance’ following initial failure in prevention, are run for a maximum of 50 years after the starting point (same as in the previous numerical studies). We also assume, as before that potential therapeutic resistance mechanisms to all intervention types are identical.

Figure 5 presents the comparative outcomes. When prevention starts at (or tumour resection misses) relatively large cancer cell populations (one million cells), only small comparative gains occur from higher cell arrest in outright treatment success (Figure 5A), whereas interventions starting at much smaller cancer cell numbers (10,000), results in considerably greater outright success (Figure 5B). Looking at situations of relapse only for prevention vs. post-diagnostic intervention, the former generally results in superior outcomes in terms of delaying tumour growth, particularly for large residual cell populations (*cf* Figures 5C and 5D). In contrast, for lower numbers of residual cells, some post-diagnostic resected tumours in the sample will be initially resistance free (Figure 5 – figure supplement 1B). This, together with fewer accumulated drivers in the highest driver subclones contribute to improved outcomes should relapse occur (Figure 5D) and overall treatment success at sufficiently high intensities (Figures 5B,F). Importantly, resected tumours in both the prevention (when it initially fails) and post-diagnostic scenarios may contain numerous resistant cells (example of 0.25% daily cellular arrest: Figure 5 – figure supplements 2,3), but prior selection for resistance in initially failed prevention generally results in larger residual resistant cell populations than pre-therapeutic residual populations in post-diagnostic situations (filled bars, *cf* captions A and B in Figure 5 – figure supplement 2,3), but less than treatment failures following post-diagnostic resection (hatched bars, *cf* captions A and D in Figure 5 – figure supplement 2,3). Note that, as expected, secondary failures are associated with larger percentages of resistant subclones, and a shift in the distributions towards more drivers (*cf* captions C and D in Figure 5 – figure supplement 2,3).

Figures 6E,F show the distributions of detection times for all of the numerical experiments. We see that when both non-relapse (Figure 5A) and relapse (Figure 5C) are taken into account for large cancer cell populations (1 million cells), treating preventively at levels beyond *c* 0.3% arrest per day increases median delays in detection times due to outright success (i.e., survival beyond 50 years), but has no effect on the lower 95th percentile (Figure 5E). (Although not shown, arrest beyond *c* 0.6% per day does not yield further gains). In contrast, post-diagnostic intervention improves marginally beyond daily arrest levels of *c* 0.3% (Figure 5E). Figure 5F shows the corresponding results for smaller cancer cell populations (based on integrating the results in

Figures 6B and 6D), whereby a high median probability of full success is obtained $>0.2\%$ and $>0.3\%$ daily arrest, for prevention and post-diagnostic intervention, respectively (Figure 5F). Thus for both cell population levels, prevention generally results in better outcomes compared to post-diagnostic intervention.

Discussion

Maximum tolerated dose chemotherapies present numerous challenges, a major one being the selection of resistant phenotypes, which are possible precursors for relapse (41). We mathematically and numerically investigated how the intensity of an anti-cancer measure, modelled as the arresting effect on a cancer cell population, resulted in success (i.e., either eradication or long-term tumour control) or failure (tumours growing beyond a threshold indicative of a life threatening cancer). Our central result is that beyond low impact thresholds—approximated by the Darwinian fitness of the subclone with the most driver mutations—no additional control is achieved when resistant subclones are present or likely to emerge during the intervention.

We considered two contrasting scenarios. In the first, people at high risk of contracting a life threatening cancer make life-style changes or receive continuous, chemopreventive therapies, and in the second, more usual situation, a tumour is discovered, removed and the patient treated with specific cytotoxic or cytostatic chemicals and/or with radiation. We found that, as expected, to achieve a given outcome, prevention requires smaller effects on tumour populations of a given size than do post-diagnostic interventions, the latter having smaller probabilities of complete cure and shorter times to tumour relapse. Inversely and importantly, for any given cell arrest level, prevention is, on average, superior to comparable post-diagnosis interventions, even when including cases where prevention initially fails and resection and additional therapy are needed.

Specifically, based on empirical parameter estimates, we find that maximal control occurs at surprisingly low daily levels of arrest. In the example where interventions target 1 million cancer cells, these levels are c 0.6% and 0.3% for preventive and post-diagnostic interventions, respectively. That the level is higher for preventive scenarios is because effective ‘cure’ (i.e., relapse does not occur during the 50 year period assumed in our numerical experiments) is possible, especially at cell arrest levels beyond 0.3%, whereas ‘cure’ is much less probable for post-diagnostic interventions. However, should prevention initially fail and a tumour be diagnosed and resected, any residual or metastatic cells are likely to contain more resistant clones than the corresponding situation for a post-diagnostic tumour. We stress that this latter result is contingent on our assumption that the *same* mutations (and mechanisms) are responsible for resistance to both preventive interventions and post-diagnostic interventions. Should preventive and post-diagnostic measures differ substantially in their targets (and therefore resistance mechanisms), then evolved resistance to (failed) prevention could be irrelevant to the efficacy of subsequent traditional therapies.

Our results point to what is perhaps an underappreciated challenge in cancer control: low impact interventions risk being unable to control subclones with the most fitness-enhancing drivers, whereas high levels of arrest risk selecting for resistance (Figure 6). Future models should investigate these contingencies more extensively for alternative assumptions and a range of parameterizations for specific cancer types. Below we discuss challenges to cancer management for both preventive and post-diagnostic scenarios.

Preventive interventions

Whereas primary prevention is becoming an increasingly significant approach in reducing risk of certain cancers (e.g. (42)), chemopreventive therapies more generally are uncommon, despite empirical support for their effects (15). Several theoretical and *in vitro* experimental studies indicate that chemoprevention can reduce risks of life threatening cancers. For example, Silva and colleagues (43) parameterized computational models to show how low doses of verapamil and 2-deoxyglucose could be administered adaptively to promote longer tumour progression times. These drugs are thought to increase the costs of resistance and the competitive impacts of sensitive cells on resistant cancer cell subpopulations. However, some of the most promising results have come from studies employing non-steroidal anti-inflammatory drugs (NSAIDs), including experiments (44), investigations of their molecular effects (45,46), and their use (47). For example, Ibrahim and co-workers (44) studied the action of NSAIDs and specifically sodium bicarbonate in reducing prostate tumours in male TRAMP mice (*i.e.* an animal model of transgenic adenocarcinoma of the mouse prostate). They showed that mice commencing the treatment at 4 weeks of age had significantly smaller tumour masses, and that more survived to the end of the experiment than either the controls or those mice commencing the treatment at an older age. Kostadinov and colleagues (45) showed how NSAID use in a sample of people with Barrett's oesophagus is associated with reductions in somatic genomic abnormalities and their growth to detectable levels. It is noteworthy that it is not known to what extent reductions in cancer progression under NSAIDs is due to either cytotoxic or cytostatic effects, or both. Although we do not explicitly model cytotoxic or cytostatic impacts, therapies curbing net growth rates, but maintaining them at or above zero, could be interpreted as resulting from the action of either cytotoxic and/or cytostatic processes. In contrast, therapies reducing net growth rates substantially below zero necessarily have a cytotoxic component. Our model, or modifications of it to explicitly include cytotoxic and cytostatic effects, could be used in future research to make predictions about optimal dose and start times to achieve acceptable levels of tumour control (or, e.g., the probability of a given tumour size and heterogeneity level by a given age).

Decisions whether or not to employ specific chemopreventive therapies carry with them the risk of a poorer outcome than would have been the case had another available strategy (or no treatment at all) been adopted (48). This issue is relevant to situations where alterations in life-style, removal or treatment of pre-cancerous lesions, or medications potentially result in

unwanted side effects or induce new invasive neoplasms (*e.g.*, (49)). Chemopreventive management prior to clinical detection would be most appropriate for individuals with genetic predispositions, familial histories, elevated levels of specific biomarkers, or risk-associated behaviours or life-styles (15,17,18,50,51). Importantly, our approach presupposes that the danger a nascent, growing tumour presents is proportional to its size and (implicitly, all else being equal) a person's age. Due caution is necessary in interpreting our results, since studies have argued that metastatic potential rather than tumour size may be a better predictor of future survival (52,53,54). However, given the expectation that prevention typically confronts smaller, less heterogeneous neoplasms, which are less likely to have resistant clones and to have metastasised (18,55), supports our basic conclusion that prevention is generally a superior strategy in terms of cancer-free survival to post-diagnostic intervention.

Post-diagnostic interventions

Over the past decade, several alternative approaches to MTD have been proposed, where the objective is to manage rather than eradicate tumours (*e.g.*, (8,12,13,14,56,57)). Tumour management attempts to limit cancer growth, metastasis, and reduce the probability of obtaining resistance mutations through, for example, micro-environmental modification or through competition with non-resistant cancer cell populations or with healthy cells. These approaches usually involve clinically diagnosed cancers: either inoperable tumours or residual or metastatic cancers after tumour excision. In the former situation, tumours are typically large enough in size to contain numerous resistance mutations. In many, if not most, cases these neoplasms will have metastasized, meaning greater variability both in terms of phenotypes and potential resistance to chemotherapies, and in penetrance of therapeutic molecules to targeted tumour cells (58,59). In contrast, the latter situation involves smaller, residual or metastatic cancer cell populations, but composed of high frequencies of resistant variants or dormant cells (58). According to our results, both scenarios are likely to involve populations with large numbers of accumulated driver mutations (or, although not considered in our study, fewer driver mutations, but each with larger selective effect), which ostensibly contribute to the speed of relapse. Thus, management of clinically detected tumours need not only limit the proliferation and spread of refractory subpopulations (Figure 2 and Figure 2 - supplement 1), but should also aim to control the growth of multi-driver subclones (Figure 2 – figure supplement 1B). In other words, in addition to actual resistance mutations ($j = 1$), subclones with q drivers, such that $q s \gg \sigma$ will be effectively resistant to therapeutic interventions.

We therefore suggest that the frequency distribution of driver mutations and the distribution of resistant subclones within a heterogeneous cancer cell population could be used to instruct decisions of the time course of treatment levels, with the aims of curbing tumour growth, metastasis, and resistance. We found that tumours typically achieve several additional driver mutations by the time they reach detection (Figure 3A,C; Figure 3 – figure supplement 1A,C;

Figure 5 – figure supplement 2,3), which approximates certain estimates (60), but falls short of others (61).

Conclusion

Our results indicate that the two most important variables in determining therapeutic outcome are (1) the size of the initial cancer cell population (i.e. when prevention commences and/or post-diagnosis, following resection), and (2) associated tumour heterogeneity in terms of accumulated drivers and the presence of resistance phenotypes. This highlights the importance of biomarkers as accurate indicators of otherwise undetectable malignancies (62), and the accurate assessment of local or distant metastases (63). We suggest that if order-of-magnitude estimates of cell populations and intra-tumour heterogeneity are possible, then low dose, continuous, constant approaches could be established that lower or even minimize risks of the emergence of future, life-threatening cancers. According to our model such options will generally be superior to more aggressive chemotherapies if therapeutic resistance is a risk factor.

The framework proposed here is sufficiently general to portray major events in different types of cancer with emphasis on solid tumours. However, some aspects of cancerous tumour growth are considered only implicitly and further research is required to formulate more realistic models to include, for example, spatial aspects of tumour growth (64), competition/cooperation between different subclones (65), combinational (multidrug) resistance (2,66), drug-addiction, observed for example in certain melanomas (39), or advantageous resistant mutations, observed in some leukemias (67). Moreover, future studies should also investigate alternatives to the traditional post-diagnostic therapeutic scenarios considered here (e.g., molecularly targeted therapies (68)). Our study nevertheless predicts that the main hurdle to post-diagnostic MTD interventions remains resistant subclones, since beyond minimal impacts on the order of 0.3% per day for the *larger* of the two residual or metastatic cell populations simulated here (which are still very small by clinical diagnostic standards – $c\ 1\ \text{mm}^3$), increased therapeutic intensity selects disproportionally for resistance and has negligible benefits in terms of delaying life-threatening cancers.

Acknowledgments

The authors are grateful to Athena Aktipis, Daniel Fisher, Sylvain Gandon, Urszula Hibner, Patrice Lassus, Carlo Maley, Ville Mustonen and Robert Noble for discussions and helpful remarks. All calculations were made using programs, written in C, and the free, open-source statistical package R (69). The colour palette for figures was adopted from (70). Code for all calculations, and for producing all of the figures, is available at (71) and can be used freely for non-commercial purposes. The work was made possible by the facilities of the Shared Hierarchical Academic Research Computing Network (SHARCNET:www.sharcnet.ca) and Compute/Calcul Canada. ARA was supported by CNRS Interdisciplinary postdoctoral program.

MEH thanks ITMO "Physique Cancer" (CanEvolve PC201306), ANR (EvoCan ANR-13-BSV7-0003-01) and PICS (PICS05313) for financial support.

References

[1] Wodarz D, Komarova N. 2007 Can loss of apoptosis protect against cancer? *Trends Genet* **23**: 232–237.

[doi:10.1016/j.tig.2007.03.005](https://doi.org/10.1016/j.tig.2007.03.005)

[2] Bozic I, Reiter JG, Allen B, Antal T, Chatterjee K, Shah P, Moon YS, Yaqubie A, Kelly N, Le DT, Lipson EJ, Chapman PB, Diaz LAJ, Vogelstein B, Nowak MA. 2013 Evolutionary dynamics of cancer in response to targeted combination therapy. *eLife* **2**: e00747.

[doi:10.7554/eLife.00747](https://doi.org/10.7554/eLife.00747)

[3] Marusyk A, Almendro V, Polyak K. 2012 Intra-tumour heterogeneity: a looking glass for cancer? *Nat Rev Cancer* **12**: 323–334.

[doi:10.1038/nrc3261](https://doi.org/10.1038/nrc3261)

[4] McFarland CD, Korolev KS, Kryukov GV, Sunyaev SR, Mirny LA. 2013 Impact of deleterious passenger mutations on cancer progression. *Proc Natl Acad Sci USA* **110**: 2910–2915.

[doi:10.1073/pnas.1213968110](https://doi.org/10.1073/pnas.1213968110)

[5] Michor F, Hughes TP, Iwasa Y, Branford S, Shah NP, Sawyers CL, Nowak MA. 2005 Dynamics of chronic myeloid leukaemia. *Nature* **435**: 1267–1270.

[doi:10.1038/nature03669](https://doi.org/10.1038/nature03669)

[6] Huijben S, Bell AS, Sim DG, Tomasello D, Mideo N, Day T, Read AF. 2013 Aggressive chemotherapy and the selection of drug resistant pathogens. *PLoS Pathog* **9**: e1003578.

[doi:10.1371/journal.ppat.1003578](https://doi.org/10.1371/journal.ppat.1003578)

[7] Foo J, Michor F. 2009 Evolution of resistance to targeted anti-cancer therapies during continuous and pulsed administration strategies. *PLoS Comput Biol* **5**, e1000557.

[doi:10.1371/journal.pcbi.1000557](https://doi.org/10.1371/journal.pcbi.1000557)

[8] Foo J, Michor F. 2010 Evolution of resistance to anti-cancer therapy during general dosing schedules. *J Theor Biol* **263**, 179–188.

[doi:10.1016/j.jtbi.2009.11.022](https://doi.org/10.1016/j.jtbi.2009.11.022)

[9] Lorz A, Lorenzi T, Hochberg ME, Clairambault J, Perthame B. 2013 Populational adaptive evolution, chemotherapeutic resistance and multiple anti-cancer therapies *ESAIM: Math Model Numer Anal* **47**, 377–399.

525 [10] Turke AB, Zejnullahu K, Wu YL, Song Y, Dias-Santagata D, Lifshits E, Toschi L,
526 Rogers A, Mok T, Sequist L, Lindeman NI, Murphy C, Akhavanfard S, Yeap BY, Xiao Y,
527 Capelletti M, Iafrate AJ, Lee C, Christensen JG, Engelman JA, Janne PA. 2010 Preexistence
528 and clonal selection of MET amplification in EGFR mutant NSCLC. *Cancer Cell* **17**: 77–88.
529 [doi:10.1016/j.ccr.2009.11.022](https://doi.org/10.1016/j.ccr.2009.11.022)

530 [11] Kouyos RD, Metcalf CJE, Birger R, Klein EY, Abel zur Wiesch P, Ankomah P,
531 Arinaminpathy N, Bogich TL, Bonhoeffer S, Brower C, Chi-Johnston G, Cohen T, Day T,
532 Greenhouse B, Huijben S, Metlay J, Mideo N, Pollitt LC, Read AF, Smith DL, Standley C,
533 Wale N, Grenfell B. 2014 The path of least resistance: aggressive or moderate treatment?
534 *Proc Biol Sci* **281**: 20140566.
535 [doi:10.1098/rspb.2014.0566](https://doi.org/10.1098/rspb.2014.0566)

536 [12] Komarova NL, Wodarz D. 2005 Drug resistance in cancer: principles of emergence and
537 prevention. *Proc Natl Acad Sci USA* **102**: 9714–9719.
538 [doi:10.1073/pnas.0501870102](https://doi.org/10.1073/pnas.0501870102)

539 [13] Gatenby RA, Brown JS, Vincent T. 2009 Lessons from applied ecology: cancer control
540 using an evolutionary double bind. *Cancer Res* **69**: 7499–7502.
541 [doi:10.1158/0008-5472.CAN-09-1354](https://doi.org/10.1158/0008-5472.CAN-09-1354)

542 [14] Maley CC, Reid BJ, Forrest S. 2004 Cancer prevention strategies that address the
543 evolutionary dynamics of neoplastic cells: simulating benign cell boosters and selection for
544 chemosensitivity. *Cancer Epidemiol Biomarkers Prev* **13**: 1375–1384.

545 [15] William WNJ, Heymach JV, Kim ES, Lippman SM. 2009 Molecular targets for cancer
546 chemoprevention. *Nat Rev Drug Discov* **8**: 213–225.
547 [doi:10.1038/nrd2663](https://doi.org/10.1038/nrd2663)

548 [16] Etzioni R, Urban N, Ramsey S, McIntosh M, Schwartz S, Reid B, Radich J, Anderson G,
549 Hartwell L. 2003 The case for early detection. *Nat Rev Cancer* **3**: 243–252.
550 [doi:10.1038/nrc1041](https://doi.org/10.1038/nrc1041)

551 [17] Lippman SM, Lee JJ. 2006 Reducing the “risk” of chemoprevention: defining and
552 targeting high risk – 2005 AACR Cancer Research and Prevention Foundation Award
553 Lecture. *Cancer Res* **66**: 2893–2903.
554 [doi:10.1158/0008-5472.CAN-05-4573](https://doi.org/10.1158/0008-5472.CAN-05-4573)

555 [18] Hochberg ME, Thomas F, Assenat E, Hibner U. 2013 Preventive evolutionary medicine
556 of cancers. *Evol Appl* **6**: 134–143.
557 [doi:10.1111/eva.12033](https://doi.org/10.1111/eva.12033)

558 [19] Doll R, Peto R. 1976 Mortality in relation to smoking: 20 years’ observations on male
559 British doctors. *Br Med J*, **2**: 1525–1536.

- 560 [20] Steward WP, Brown K. 2013 Cancer chemoprevention: a rapidly evolving field. *Br J*
561 *Cancer* **109**: 1–7.
562 [doi:10.1038/bjc.2013.280](https://doi.org/10.1038/bjc.2013.280)
- 563 [21] Bissell MJ, Hines WC. 2011 Why don't we get more cancer? A proposed role of the
564 microenvironment in restraining cancer progression. *Nat Med* **17**: 320–329.
565 [doi:10.1038/nm.2328](https://doi.org/10.1038/nm.2328)
- 566 [22] Greaves M. 2014 Does everyone develop covert cancer? *Nat Rev Can* **14**: 209–210.
567 [doi:10.1038/nrc3703](https://doi.org/10.1038/nrc3703)
- 568 [23] Vogelstein B, Papadopoulos N, Velculescu VE, Zhou S, Diaz LAJ, Kinzler KW. 2013
569 Cancer genome landscapes. *Science* **339**: 1546–1558.
570 [doi:10.1126/science.1235122](https://doi.org/10.1126/science.1235122)
- 571 [24] Gillies RJ, Flowers CI, Drukteinis JS, Gatenby RA. 2012 A unifying theory of
572 carcinogenesis, and why targeted therapy doesn't work. *Eur J Radiol* **81**(Suppl 1): S48–50.
573 [doi:10.1016/S0720-048X\(12\)70018-9](https://doi.org/10.1016/S0720-048X(12)70018-9)
- 574 [25] Wu X, Lippman SM. 2011 An intermittent approach for cancer chemoprevention. *Nat*
575 *Rev Cancer* **11**, 879–885.
576 [doi:10.1038/nrc3167](https://doi.org/10.1038/nrc3167)
- 577 [26] Gerstung M, Eriksson N, Lin J, Vogelstein B, Beerenwinkel N. 2011 The temporal order
578 of genetic and pathway alterations in tumorigenesis. *PLoS One*. **6**: e27136.
579 [doi:10.1371/journal.pone.0027136](https://doi.org/10.1371/journal.pone.0027136)
- 580 [27] Bozic I, Antal T, Ohtsuki H, Carter H, Kim D, Chen S, Karchin R, Kinzler KW,
581 Vogelstein B, Nowak MA. 2010 Accumulation of driver and passenger mutations during
582 tumor progression. *Proc Natl Acad Sci USA* **107**: 18545–18550.
583 [doi:10.1073/pnas.1010978107](https://doi.org/10.1073/pnas.1010978107)
- 584 [28] Reiter JG, Bozic I, Allen B, Chatterjee K, Nowak MA. 2013 The effect of one
585 additional driver mutation on tumor progression. *Evol Appl* **6**: 34–45.
586 [doi:10.1111/eva.12020](https://doi.org/10.1111/eva.12020)
- 587 [29] Beerenwinkel N, Schwarz RF, Gerstung M, Markowitz F. 2015 Cancer evolution:
588 mathematical models and computational inference. *Syst Biol* **64**(1): e1–25.
589 [doi:10.1093/sysbio/syu081](https://doi.org/10.1093/sysbio/syu081)
- 590 [30] Krapivsky PL, Redner S, Ben-Naim EA. 2010 Kinetic View of Statistical Physics
591 *Cambridge: Cambridge University Press*.
- 592 [31] Gardiner CW. 2004 Handbook of Stochastic Methods, 3rd edn. *Springer*.

593 [32] Antal T, Krapivsky PL. 2011 Exact solution of a two-type branching process: models of
594 tumor progression. *J Stat Mech Theory Exp* **2011**(08): P08018.
595 [doi:10.1088/1742-5468/2011/08/P08018](https://doi.org/10.1088/1742-5468/2011/08/P08018)

596 [33] Kessler DA, Levine H. 2013 Large population solution of the stochastic Luria-Delbruck
597 evolution model. *Proc Natl Acad Sci USA* **110**: 11682–11687.
598 [doi:10.1073/pnas.1309667110](https://doi.org/10.1073/pnas.1309667110)

599 [34] Baake E, Wagner H. 2001 Mutation-selection models solved exactly with methods of
600 statistical mechanics. *Genet Res* **78**: 93-117.

601 [35] Saakian DB, Hu CK. 2006 Exact solution of the Eigen model with general fitness
602 functions and degradation rates. *Proc Natl Acad Sci USA* **103**: 4935–4939.
603 [doi:10.1073/pnas.0504924103](https://doi.org/10.1073/pnas.0504924103)

604 [36] Durrett R. 2014 Exponentially growing cell populations. *Unpublished notes*.
605 <http://www.math.duke.edu/~rtd/cmodels/bp.pdf>

606 [37] Athreya KB, Ney PE. 1972 Branching processes. *Springer-Verlag*.

607 [38] Iwasa Y, Nowak MA, Michor F. 2006 Evolution of resistance during clonal expansion.
608 *Genetics* **172**: 2557–2566.
609 [doi:10.1534/genetics.105.049791](https://doi.org/10.1534/genetics.105.049791)

610 [39] Das Thakur M, Salangsang F, Landman AS, Sellers WR, Pryer NK, Levesque MP, Dummer
611 R, McMahon M, Stuart DD. 2013 Modelling vemurafenib resistance in melanoma reveals a
612 strategy to forestall drug resistance. *Nature* **494**: 251–255.
613 [doi:10.1038/nature11814](https://doi.org/10.1038/nature11814)

614 [40] Fischer A, Vázquez-García I, Mustonen V. 2015 The value of monitoring to control
615 evolving populations. *Proc Acad Sci USA* **112**(4): 1007–1012.
616 [doi:10.1073/pnas.1409403112](https://doi.org/10.1073/pnas.1409403112)

617 [41] Gerlinger M, Swanton C. 2010 How Darwinian models inform therapeutic failure initiated
618 by clonal heterogeneity in cancer medicine. *Br J Cancer* **103**: 1139–1143.
619 [doi:10.1038/sj.bjc.6605912](https://doi.org/10.1038/sj.bjc.6605912)

620 [42] Colditz GA, Bohlke K. 2014 Priorities for the primary prevention of breast cancer. *CA*
621 *Cancer J Clin* **64**: 186–194.
622 [doi:10.3322/caac.21225](https://doi.org/10.3322/caac.21225)

623 [43] Silva AS, Kam Y, Khin ZP, Minton SE, Gillies RJ, Gatenby RA. 2012 Evolutionary
624 approaches to prolong progression-free survival in breast cancer. *Cancer Res* **72**: 6362–6370.
625 [doi:10.1158/0008-5472.CAN-12-2235](https://doi.org/10.1158/0008-5472.CAN-12-2235)

626 [44] Ibrahim-Hashim A, Cornnell HH, Abrahams D, Lloyd M, Bui M, Gillies RJ, Gatenby
627 RA. 2012 Systemic buffers inhibit carcinogenesis in TRAMP mice. *J Urol* **188**: 624–631.
628 [doi:10.1016/j.juro.2012.03.113](https://doi.org/10.1016/j.juro.2012.03.113)

629 [45] Kostadinov RL, Kuhner MK, Li X, Sanchez CA, Galipeau PC, Paulson TG, Sather CL,
630 Srivastava A, Odze RD, Blount PL, Vaughan TL, Reid BJ, Maley CC. 2013 NSAIDs modulate
631 clonal evolution in Barrett’s esophagus. *PLoS Genet* **9**: e1003553.
632 [doi:10.1371/journal.pgen.1003553](https://doi.org/10.1371/journal.pgen.1003553)

633 [46] Galipeau PC, Li X, Blount PL, Maley CC, Sanchez CA, Odze RD, Ayub K, Rabinovitch
634 PS, Vaughan T. L, Reid, B. J. 2007 NSAIDs modulate CDKN2A, TP53, and DNA content risk
635 for progression to esophageal adenocarcinoma. *PLoS Med* **4**: e67.
636 [doi:10.1371/journal.pmed.0040067](https://doi.org/10.1371/journal.pmed.0040067)

637 [47] Cuzick J, Thorat MA, Bosetti C, Brown PH, Burn J, Cook NR, Ford LG, Jacobs EJ,
638 Jankowski JA, La Vecchia C, Law M, Meyskens F, Rothwell PM, Senn HJ, Umar A. 2015
639 Estimates of benefits and harms of prophylactic use of aspirin in the general population.
640 *Ann Oncol* **26**(1): 47–57.
641 [doi:10.1093/annonc/mdu225](https://doi.org/10.1093/annonc/mdu225)

642 [48] Esserman L, Sepucha K, Ozanne E, Hwang ES. 2004 Applying the neoadjuvant
643 paradigm to ductal carcinoma in situ. *Ann Surg Oncol* **11**: S28–36.

644 [49] Berrington de Gonzalez A, Curtis RE, Kry SF, Gilbert E, Lamart S, Berg CD, Stovall
645 M, Ron E. 2011 Proportion of second cancers attributable to radiotherapy treatment in
646 adults: a cohort study in the US SEER cancer registries. *Lancet Oncol* **12**: 353–360.
647 [doi:10.1016/S1470-2045\(11\)70061-4](https://doi.org/10.1016/S1470-2045(11)70061-4)

648 [50] Sutcliffe P, Hummel S, Simpson E, Young T, Rees A, Wilkinson A, Hamdy F, Clarke N,
649 Staffurth J. 2009 Use of classical and novel biomarkers as prognostic risk factors for localised
650 prostate cancer: a systematic review. *Health Technol Assess* **13**(iii, xi-xiii): 1–219.
651 [doi:10.3310/hta13050](https://doi.org/10.3310/hta13050)

652 [51] Hemminki, K, Li, X. 2004 Familial risk in testicular cancer as a clue to a heritable and
653 environmental aetiology. *Br J Cancer* **90**: 1765–1770.
654 [doi:10.1038/sj.bjc.6601714](https://doi.org/10.1038/sj.bjc.6601714)

655 [52] Foulkes WD, Smith IE, Reis-Filho JS. 2010 Triple-negative breast cancer. *N Engl J*
656 *Med* **363**,1938–1948
657 [doi:10.1056/NEJMra1001389](https://doi.org/10.1056/NEJMra1001389)

658 [53] Hynes RO. 2003 Metastatic potential: generic predisposition of the primary tumor or
659 rare, metastatic variants-or both? *Cell* **113**: 821–823.

660 [54] Sethi N, Kang Y. 2011 Unravelling the complexity of metastasis – molecular
661 understanding and targeted therapies. *Nat Rev Cancer* **11**: 735–748.
662 [doi:10.1038/nrc3125](https://doi.org/10.1038/nrc3125)

663 [55] Gerlinger M, McGranahan N, Dewhurst SM, Burrell RA, Tomlinson I, Swanton C. 2014
664 Cancer: evolution within a lifetime. *Annu Rev Genet* **48**: 215–236.
665 [doi:10.1146/annurev-genet-120213-092314](https://doi.org/10.1146/annurev-genet-120213-092314)

666 [56] Gatenby RA. 2009 A change of strategy in the war on cancer. *Nature* **459**: 508–509.
667 [doi:10.1038/459508a](https://doi.org/10.1038/459508a)

668 [57] Gatenby RA, Silva AS, Gillies RJ, Frieden BR. 2009 Adaptive therapy. *Cancer Res* **69**:
669 4894–4903.
670 [doi:10.1158/0008-5472.CAN-08-3658](https://doi.org/10.1158/0008-5472.CAN-08-3658)

671 [58] Klein CA, Blankenstein TJF, Schmidt-Kittler O, Petronio M, Polzer B, Stoecklein
672 NH, Riethmuller, G. 2002 Genetic heterogeneity of single disseminated tumour cells in
673 minimal residual cancer. *Lancet* **360**: 683–689.
674 [doi:10.1016/S0140-6736\(02\)09838-0](https://doi.org/10.1016/S0140-6736(02)09838-0)

675 [59] Byrne AM, Bouchier-Hayes DJ, Harmey JH. 2005 Angiogenic and cell survival functions
676 of vascular endothelial growth factor (VEGF). *J Cell Mol Med* **9**: 777–794.

677 [60] Stratton MR, Campbell PJ, Futreal PA. 2009 The cancer genome. *Nature* **458**: 719–724.
678 [doi:10.1038/nature07943](https://doi.org/10.1038/nature07943)

679 [61] Sjoblom T, Jones S, Wood LD, Parsons DW, Lin J, Barber TD, Mandelker D, Leary RJ,
680 Ptak J, Silliman N, Szabo S, Buckhaults P, Farrell C, Meeh P, Markowitz SD, Willis J,
681 Dawson D, Willson JKV, Gazdar AF, Hartigan J, Wu L, Liu C, Parmigiani G, Park BH,
682 Bachman KE, Papadopoulos N, Vogelstein B, Kinzler KW, Velculescu VE. 2006 The
683 consensus coding sequences of human breast and colorectal cancers. *Science* **314**: 268–274.
684 [doi:10.1126/science.1133427](https://doi.org/10.1126/science.1133427)

685 [62] Roukos DH, Murray S, Briasoulis E. 2007 Molecular genetic tools shape a roadmap towards
686 a more accurate prognostic prediction and personalized management of cancer. *Cancer Biology*
687 *and Therapy* **6(3)**: 308–312
688 [doi:10.4161/cbt.6.3.3994](https://doi.org/10.4161/cbt.6.3.3994)

689 [63] Pantel K, Cote R. J, Fodstad O. 1999 Detection and clinical importance of
690 micrometastatic disease. *J Natl Cancer Inst* **91**: 1113–1124.

691 [64] Orlando PA, Gatenby RA, Brown JS. 2013 Tumor evolution in space: the effects of
692 competition colonization tradeoffs on tumor invasion dynamics. *Front Oncol* **3**: 45
693 [doi:10.3389/fonc.2013.00045](https://doi.org/10.3389/fonc.2013.00045)

694 [65] Korolev KS, Xavier JB, Gore J. 2014 Turning ecology and evolution against cancer. *Nat*
695 *Rev Cancer* 14: 371–80
696 [doi:10.1038/nrc3712](https://doi.org/10.1038/nrc3712)

697 [66] Gillet J-P, Gottesman MM. 2010 Mechanisms of multidrug resistance in cancer. *Methods*
698 *Mol Biol* 596: 47–76
699 [doi:10.1007/978-1-60761-416-6_4](https://doi.org/10.1007/978-1-60761-416-6_4)

700 [67] Michor F, Hughes TP, Iwasa Y, Branford S, Shah NP, Sawyers CL, Nowak MA. 2005
701 Dynamics of chronic myeloid leukaemia. *Nature* 435: 1267–1270
702 [doi:10.1038/nature03669](https://doi.org/10.1038/nature03669)

703 [68] Yap TA. 2015 Challenges in combining novel molecularly targeted agents in cancer
704 medicine. *Annals of Oncology* 26(1): 9-11
705 [doi:10.1093/annonc/mdu483](https://doi.org/10.1093/annonc/mdu483)

706 [69] R Development Core Team. R project for statistical computing (downloaded 2013-
707 2014).
708 <http://www.r-project.org>

709 [70] Color Brewer 2: color advice for cartography.
710 <http://colorbrewer2.org>

711 [71] Code scripts used for numerical simulations.
712 <http://tiny.cc/AkhmHoch15Scripts>

713 [72] Beckman RA, Schemmann GS, Yeang CH. 2012 Impact of genetic dynamics and single-
714 cell heterogeneity on development of nonstandard personalized medicine strategies for
715 cancer. *Proc Natl Acad Sci USA* **109**: 14586–14591.
716 [doi:10.1073/pnas.1203559109](https://doi.org/10.1073/pnas.1203559109)

717 [73] Assaf M. 2010 Theory of large fluctuations in stochastic populations. *PhD thesis*,
718 *Hebrew University of Jerusalem*.
719 <http://guava.physics.uiuc.edu/~assaf/thesis.pdf>

720 [74] Elgart V, Kamenev A. 2004 Rare event statistics in reaction-diffusion systems. *Phys Rev*
721 *E Stat Nonlin Soft Matter Phys* **70**: 041106.

722 [75] Melikyan AA. 1998 Generalized characteristics of first order PDEs. *Boston, MA*:
723 *Birkhäuser*.

Tables

Table 1. Baseline parameter values used in this study. ‘Range’ includes values from previous study and employed in the present study.

Parameter	Variable	Value	Range	Ref.
Time step (cell cycle length)	T	4 days	3-4 days	(27)
Selective advantage	s	0.4%	0.1-1.0%	(27)
Cost of resistance	c	0.1%		
Mutation rate to acquire an additional driver	u	3.4×10^{-5}	10^{-7} - 10^{-2}	(27)
Mutation rate to acquire resistance	v	10^{-6}	10^{-7} - 10^{-2}	(12)
Maximal number of additional drivers	N	5 (figures 1-3) 9 (other figures)	0-9	
Initial cell population	$n(0)$	10^6 cells	-	
Pre-resistance level	κ	0.01%	-	(38)
Number of replicate numerical simulations (excluding extinctions)	-	10^6	-	
Detection threshold	M	10^9 cells	10^7 - 10^{11}	(72)

Figures

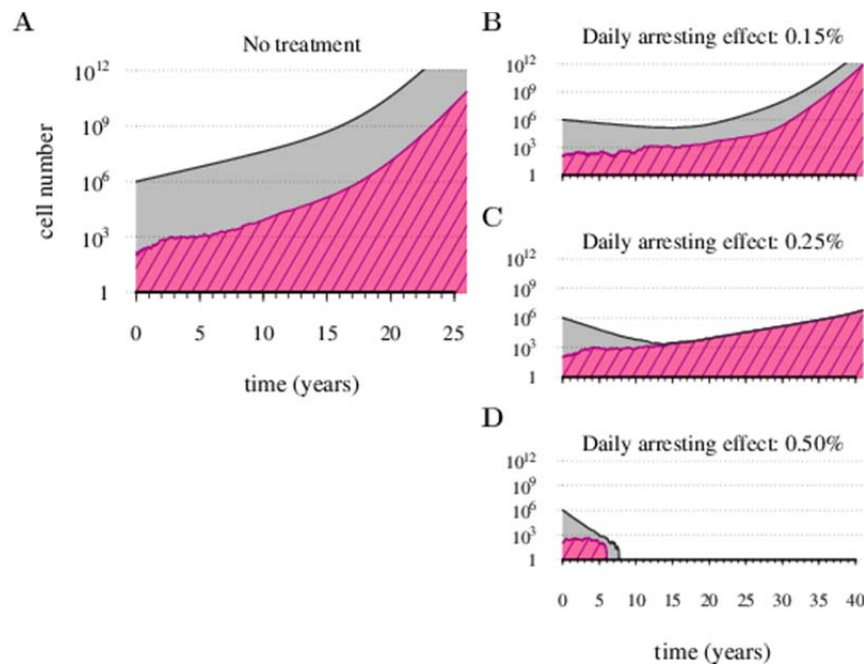


Figure 1. Treatments curb or eliminate tumours. Examples of single patient tumour growth for (A) No treatment. (B) $\sigma = 0.6\%$. (C) $\sigma = 1.0\%$. (D) $\sigma = 2.0\%$. The shaded area shows the change in total tumour size and the hatched area the resistant part of a tumour. Parameter values as in Table 1.

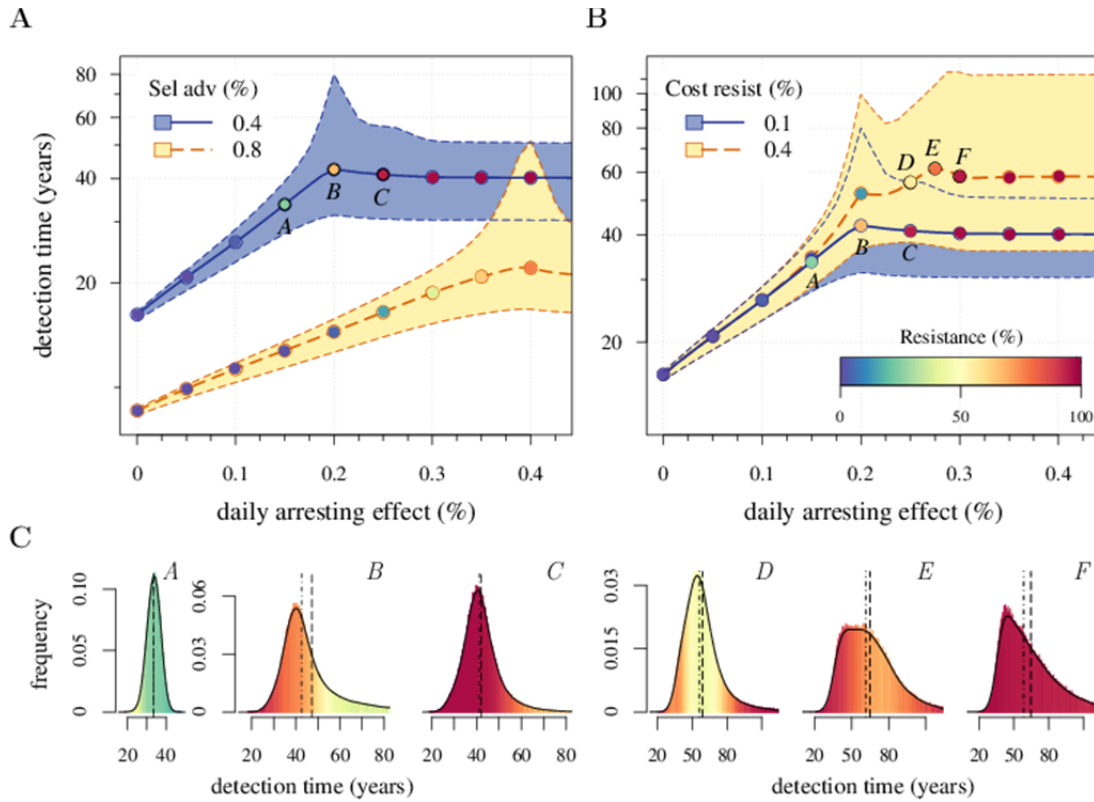


Figure 2. Treatment level affects both detection time and frequency of resistance. The median and 90% confidence intervals (shaded areas) of detection times, measured as years beyond the initiation of the preventive measure. Effects of: (A) The selective advantage and (B) The cost of resistance. (C) Samples of the distribution of detection times (in relative frequencies, adjusted for 3-month bins) for corresponding points, indicated in A and B. Dashed black line is the mean and the dashed-and-dotted line is the median. The colour-code indicates the average level of resistance in detected tumours over 3 month intervals (see inset in B). All cells $j = 0$ at $t = 0$. Parameters as in Table 1. Detection time is log-transformed in A and B. The treatment intensity σ in this and all other figures is represented as cell arrest per day ($\sigma/4$).

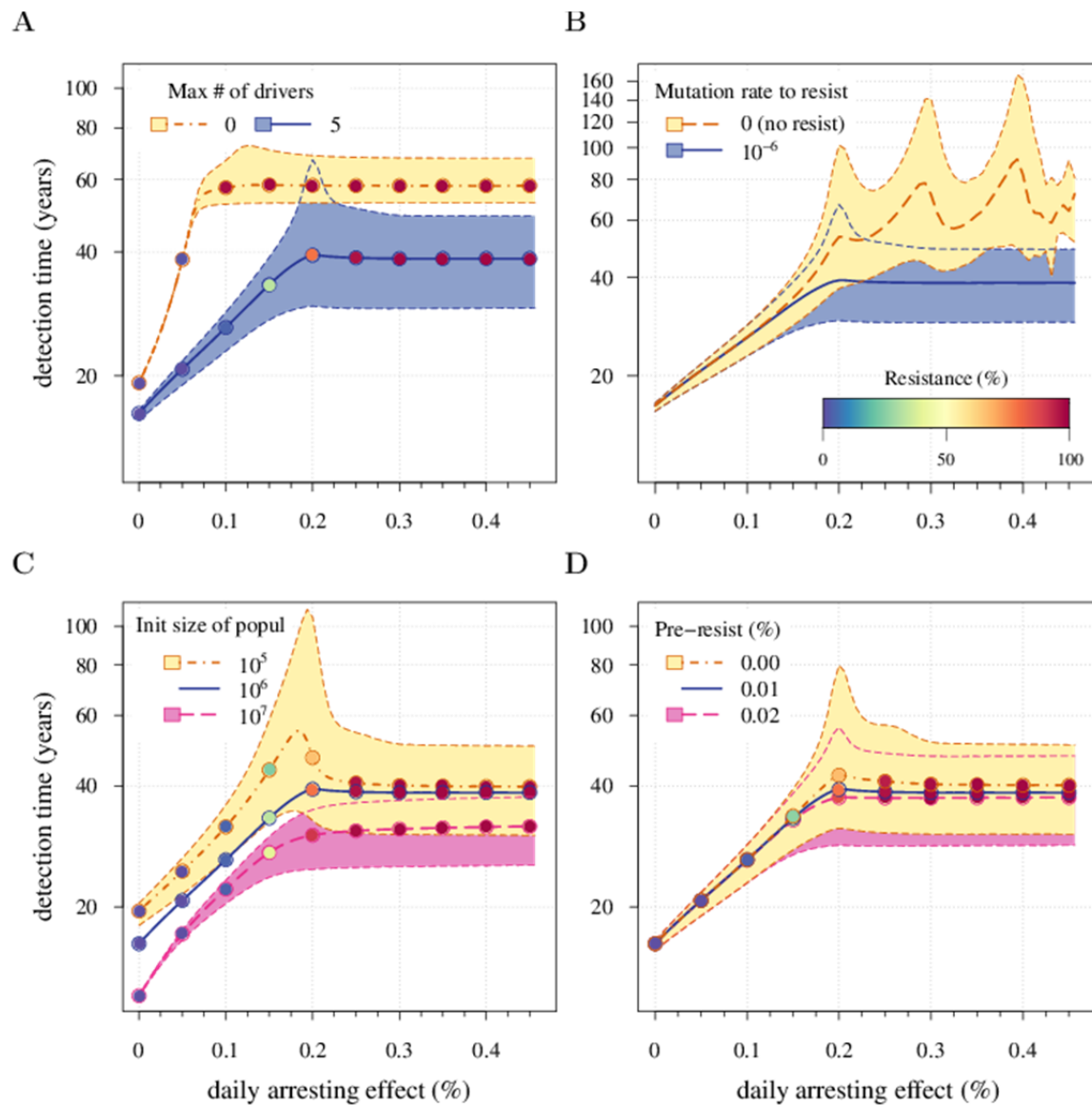


Figure 2 – figure supplement 1. Sensitivity analysis for several key parameters. (A) Maximal number of additionally accumulated drivers. (B) Presence of resistant cell-lines. (C) Initial cell number. (D) Level of initial partial resistance of a tumour. Point colour-codes indicate the average level of resistance in detected tumours over 3 month intervals (see inset in B). For simplicity, only the median is indicated in C and D for the baseline case (blue line). Lines and shading otherwise as in Figure 2. Unless otherwise stated, parameter values as in Table 1.

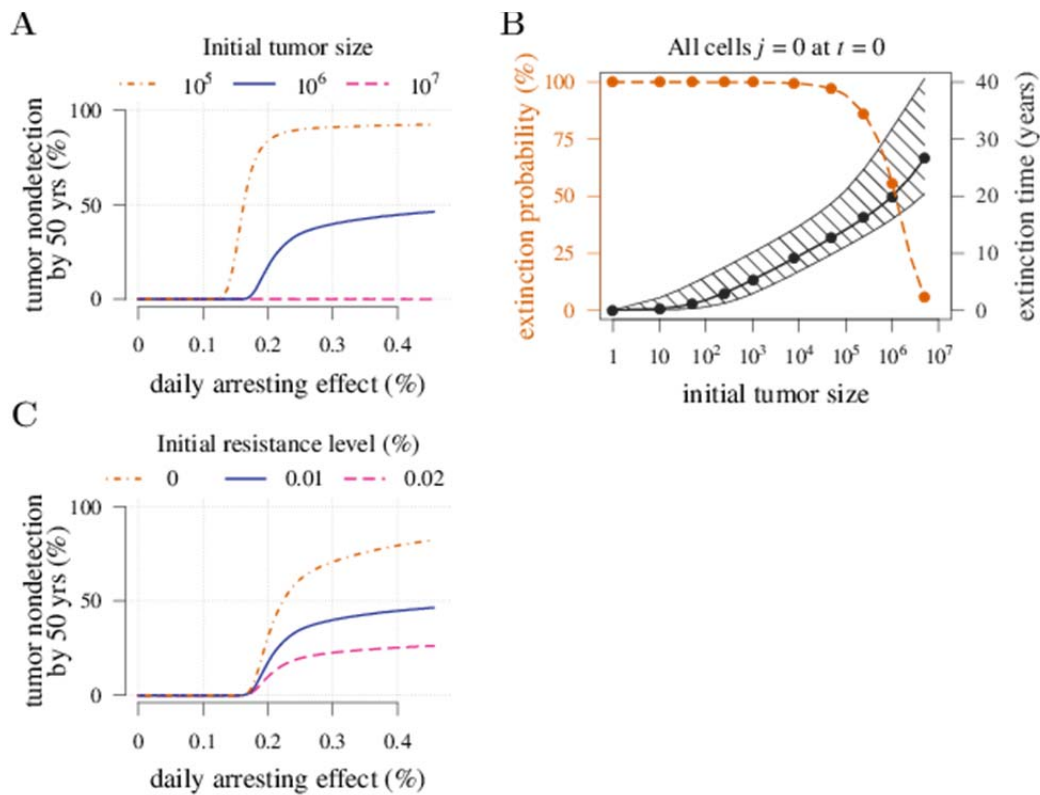


Figure 2 – figure supplement 2. Effects of initial neoplasm size (A, B) and resistance level (C) on preventive measure success. Success is defined as tumour non-detection by 50 years. Daily effect of treatment on cellular arrest is assumed to be 0.25%. Unless otherwise stated, parameter values as in Table 1.

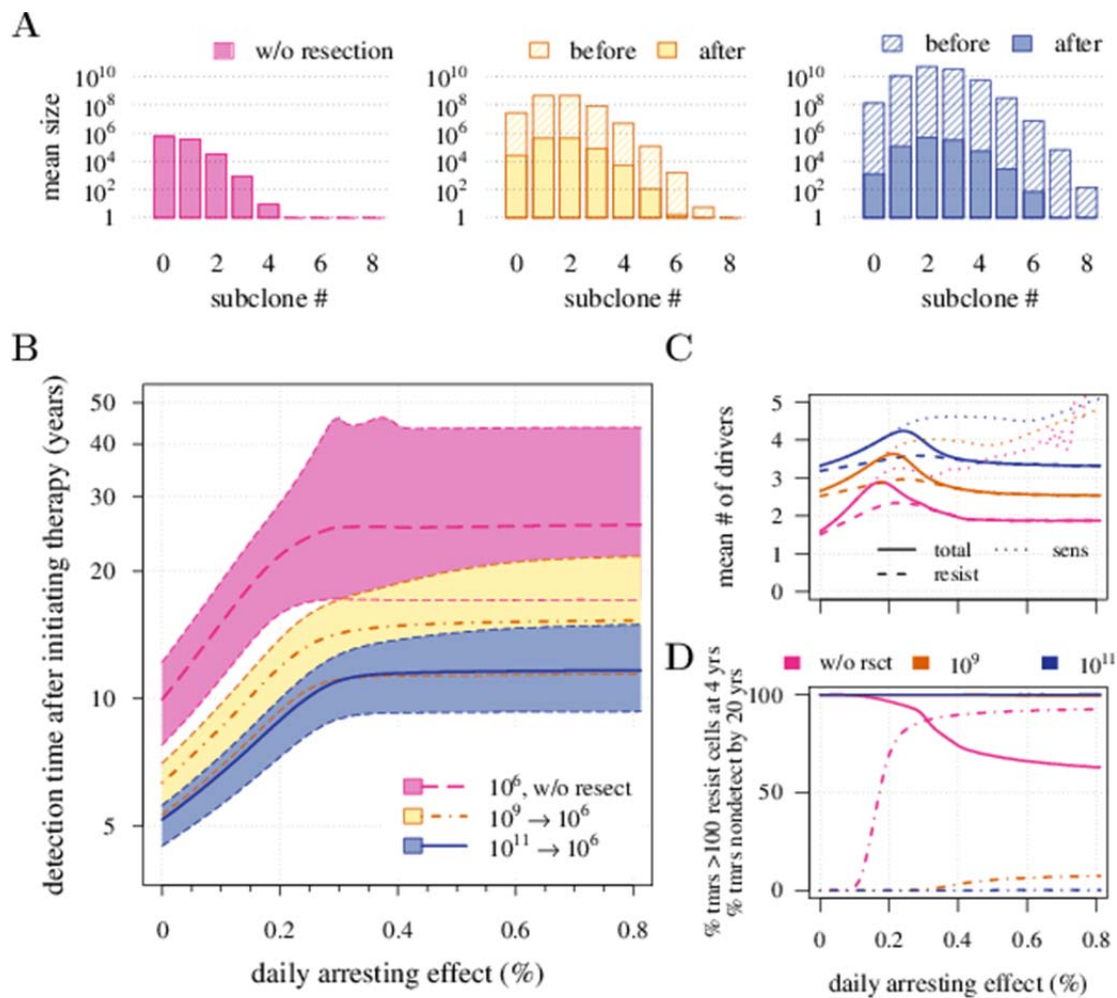


Figure 3. Effects of preventive and post-diagnostic interventions against tumours consisting of 1 million cells. (A) The distribution of mean sizes of subclones (hatched bars = before removal and solid bars = post removal). (B) The time distribution of cases in which either intervention type fails to control the tumour below the detection threshold after 50 years (thick line = median, filled area with dashed boundaries = 90% CIs) for different constant treatment intensities. (C) The mean number of accumulated drivers within a tumour at the time of detection. (D) The percentage of cases when a tumour consists of less than 100 resistant cells at 4 years post-resection (solid lines) and the percentage of cases when tumour sizes are below the detection threshold 20 years after the measure commences (dashed-and-dotted lines). Parameter values as in Table 1.

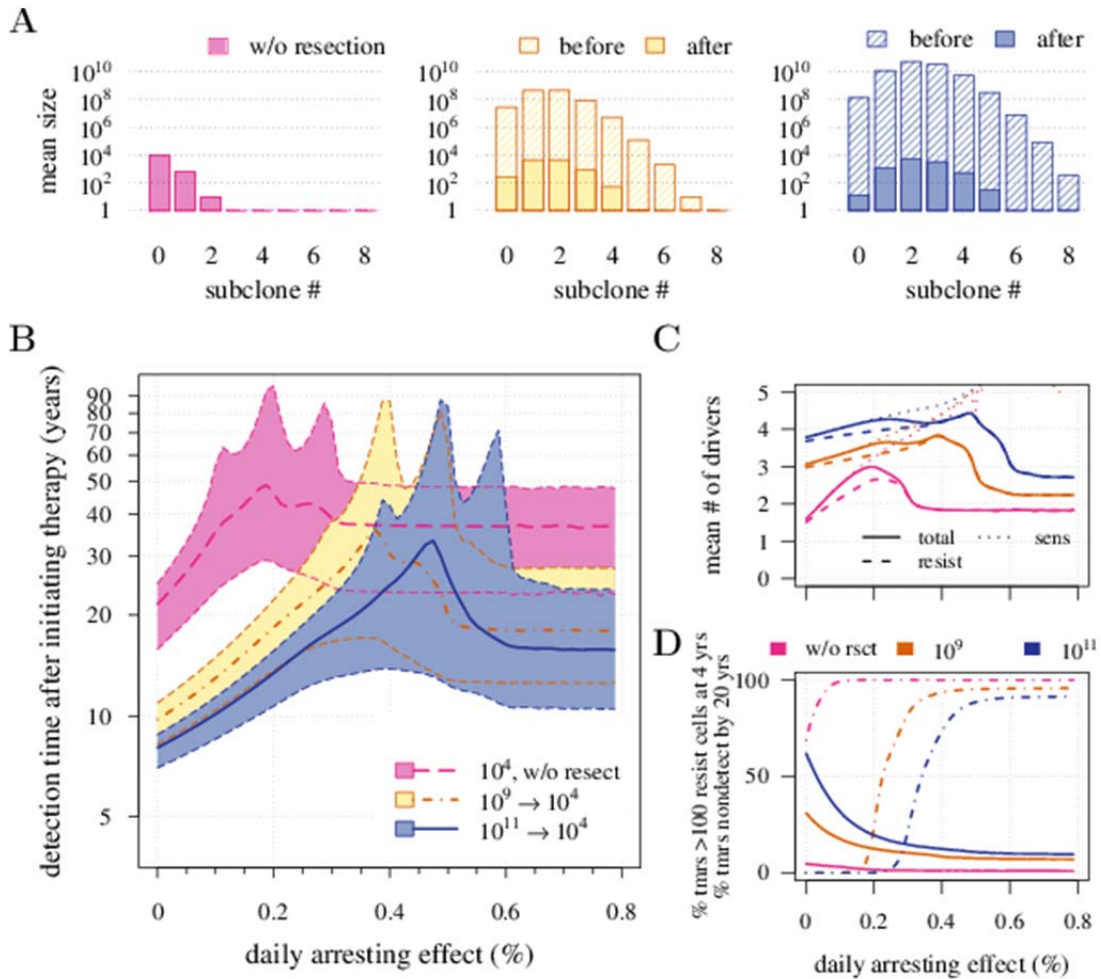


Figure 3 – figure supplement 1. Preventive versus post-diagnostic interventions. Same as Figure 3, except interventions against 10^4 cancer cells. **(A)** The distribution of mean sizes of subclones for different constant treatment intensities (hatched bars = before removal and solid bars = post removal). **(B)** The time distribution of cases in which either intervention type fails to control the tumour below the detection threshold after 50 years (thick lines = medians, shaded areas with dashed boundaries = 90% CIs). **(C)** The mean number of accumulated drivers within a tumour at the time of detection. **(D)** The percentage of cases where the tumour consists of less than 100 resistant cells at 4 years after treatment commences (solid lines), and the percentage of cases where tumour size is below the detection threshold 20 years after the measure begins (dashed-and-dotted lines). Parameter values as in Table 1.

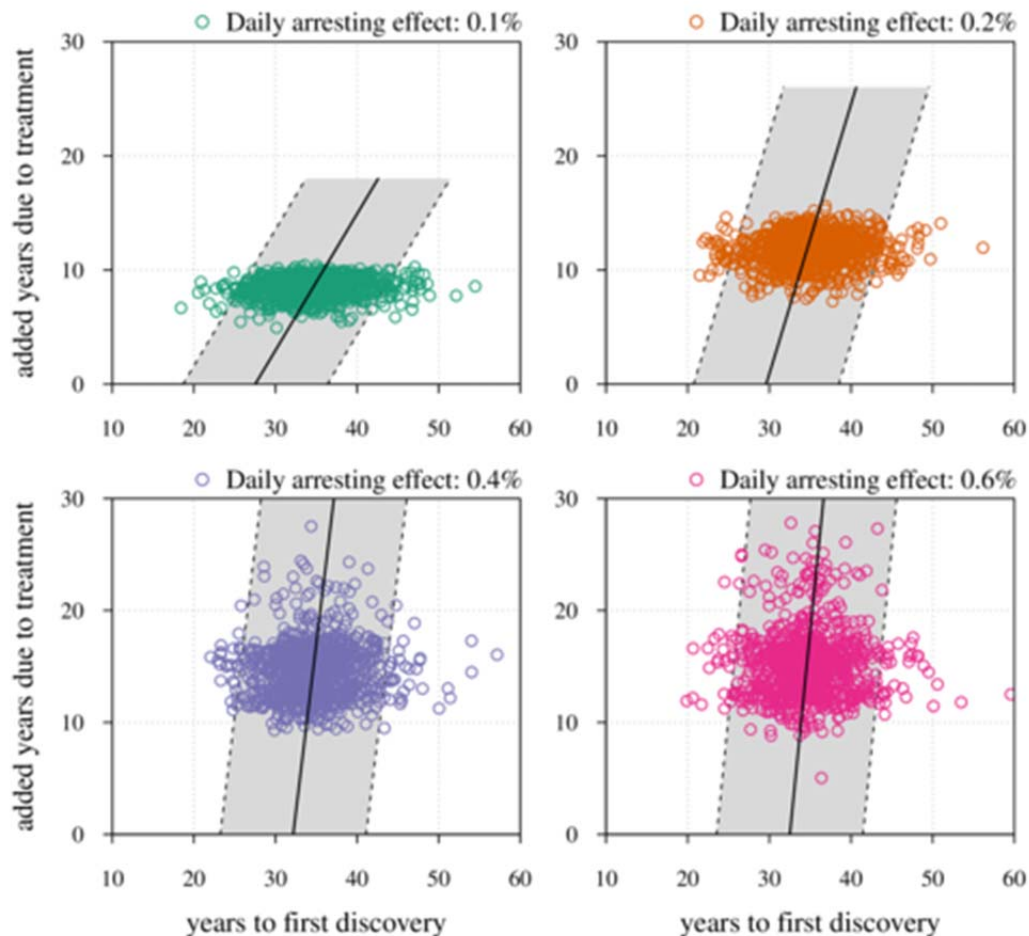


Figure 3 – figure supplement 2. Time to first discovery as a predictor of post-diagnostic treatment success. Time to tumour relapse following resection as function of the time it takes for the initial cancer cell to attain 10^9 cells (i.e., the point at which the tumour is discovered, resected and treatment begins). Each dot represents a numerical simulation from the yellow distribution in Figure 3B. Four different treatment levels are considered. Black solid line is a simple linear regression and grey area with dashed boundaries indicates extrapolation of high and low bounds accounting for 95% of observations (prediction interval). Parameters as in Table 1.

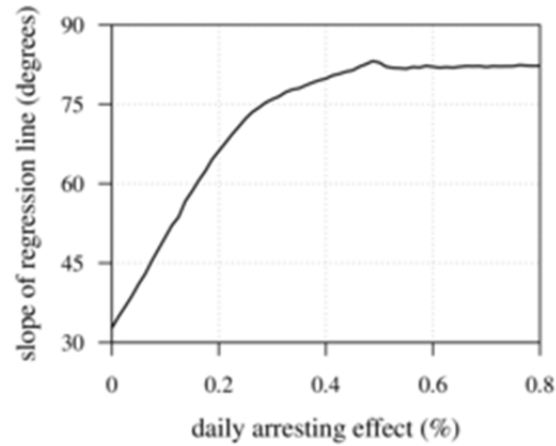


Figure 3 – figure supplement 3. Time to tumour discovery is more predictive of post-diagnostic therapeutic outcome for lower treatment levels. The slopes of regressions from numerical experiments for different treatment levels of time to tumour relapse following resection as a function of the time it takes for the initial cancer cell to attain 10^9 cells. See Figure 3 – figure supplement 2 for details.

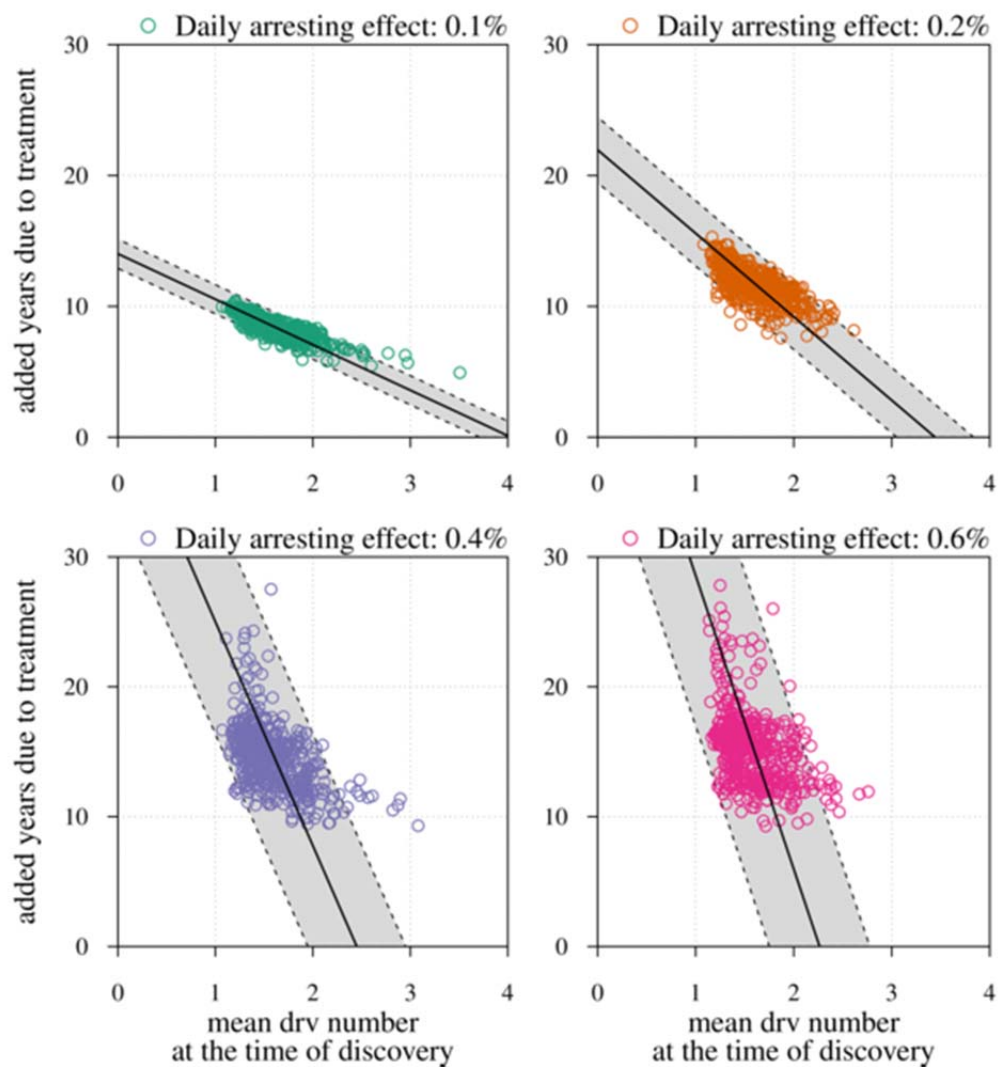
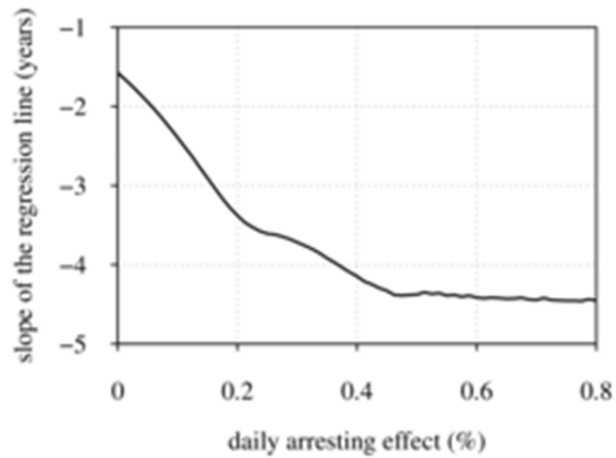


Figure 3 – figure supplement 4. Mean number of drivers in resected tumour as a predictor of post-diagnostic treatment success. See Figure 3 – figure supplement 2 for details.



797
 798 **Figure 3 – figure supplement 5. Time to tumour discovery is more predictive of post-**
 799 **diagnostic therapeutic outcome for lower treatment levels.** The slopes of regressions from
 800 numerical experiments for different treatment levels of time to tumour relapse following
 801 resection as function of the mean number of drivers in a resected tumour. See Figure 3 – figure
 802 supplement 2 for details.

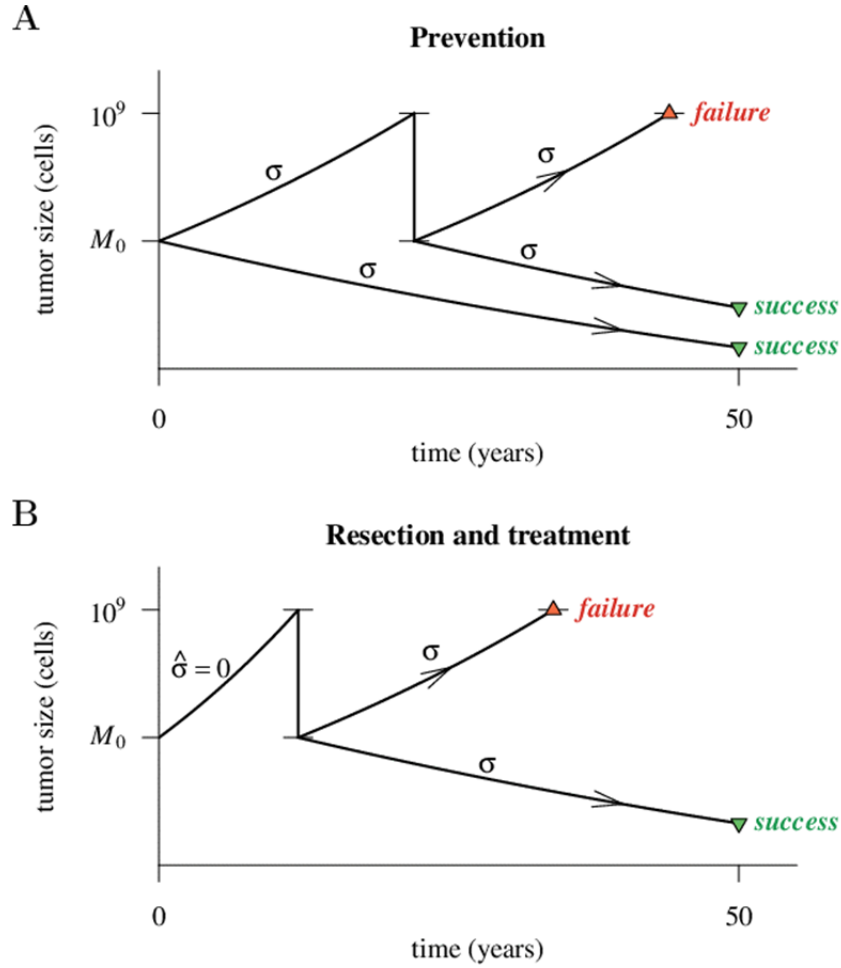


Figure 4. Hypothetical process of preventive (with a ‘second chance’) and post-diagnostic measures. A tumour is initiated by one cell and grows to size M_0 (either 10^4 or 10^6 cells in our numerical studies). Prevention (A) arrests tumour growth at intensity σ (daily level = $\sigma/4$). Should the tumour grow to 10^9 cells, it is diagnosed and resected to $M = M_0$ cells and then treated again at intensity σ . Post-diagnostic intervention (B) does not discover the growing tumour until 10^9 cells (i.e., $\sigma = \hat{\sigma} = 0$ up until this point), whereupon it is resected to $M = M_0$ cells and then treated at intensity $\sigma > 0$. Either intervention finally ‘fails’ should the tumour attain 10^9 cells a second time, no later than 50 years after the initial lesion of size M_0 . Should the tumour be eradicated or not exceed 10^9 cells by 50 years after the initial lesion, then the intervention is deemed a ‘success’.

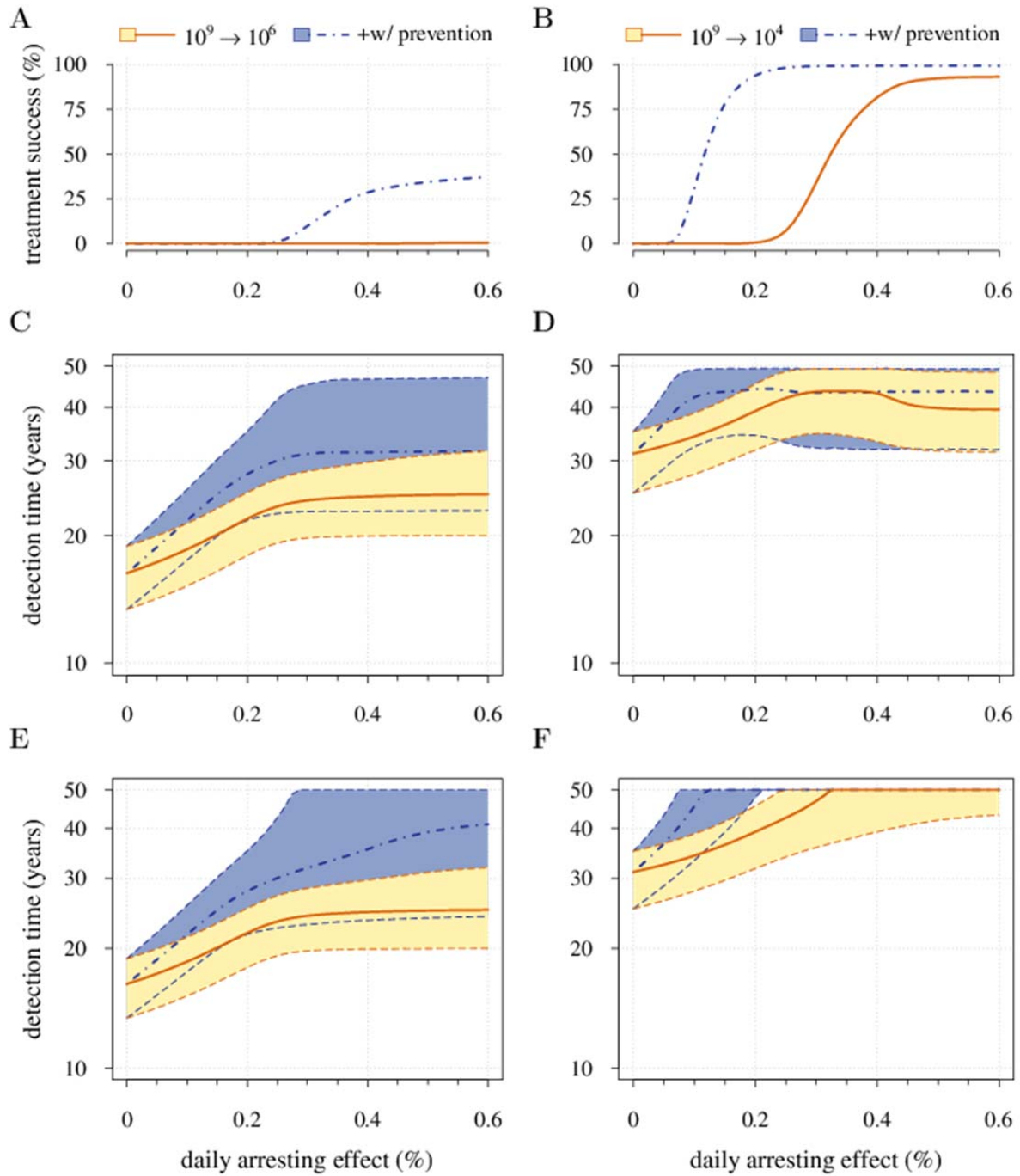


Figure 5. Comparison of preventive (blue lines and shading) and post-diagnostic (red lines, yellow shading) interventions. Tumours are either treated at $M_0 = 10^6$ cells (left panels) or $M_0 = 10^4$ cells (right panels). (A, B) Probability of treatment success, defined as the proportion of cases where the tumour remains undetected (either extinct or below 10^9 cells) by 50 years after the initial lesion of M_0 cells. (C, D) Distribution of times to relapse for treatment failures. (E, F) Distribution of detection times for all cases, including relapsed tumours and tumours remaining undetected prior to and after 50 years (detection times are assigned to 50 years in the latter case). Parameters as in Table 1. See Figure 3 for details.

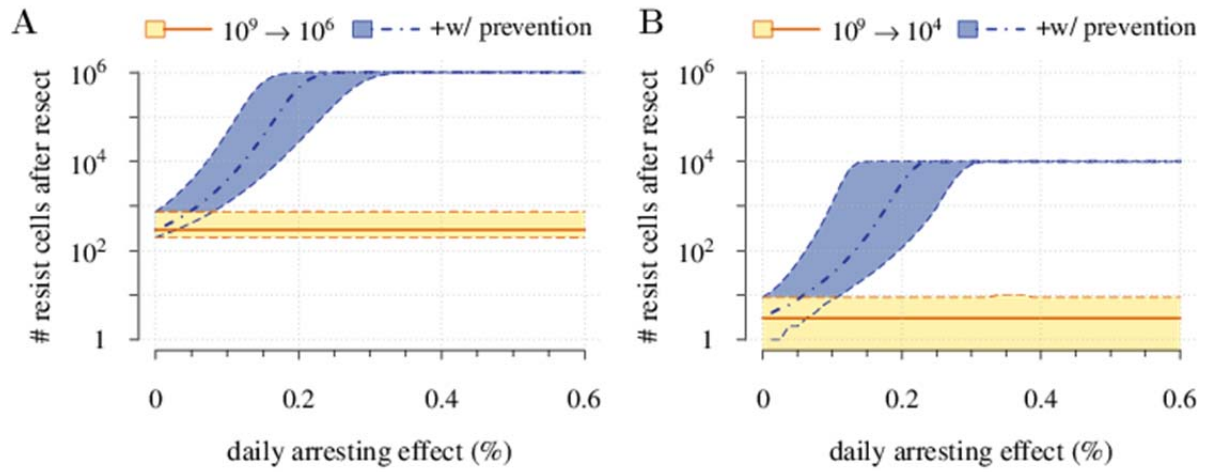


Figure 5 – figure supplement 1. Resistant cell populations after initial failure (red lines and yellow shading = population following resection). Tumours are either treated at $M_0 = 10^6$ cells (A) or $M_0 = 10^4$ cells (B). Parameter values as in Table 1.

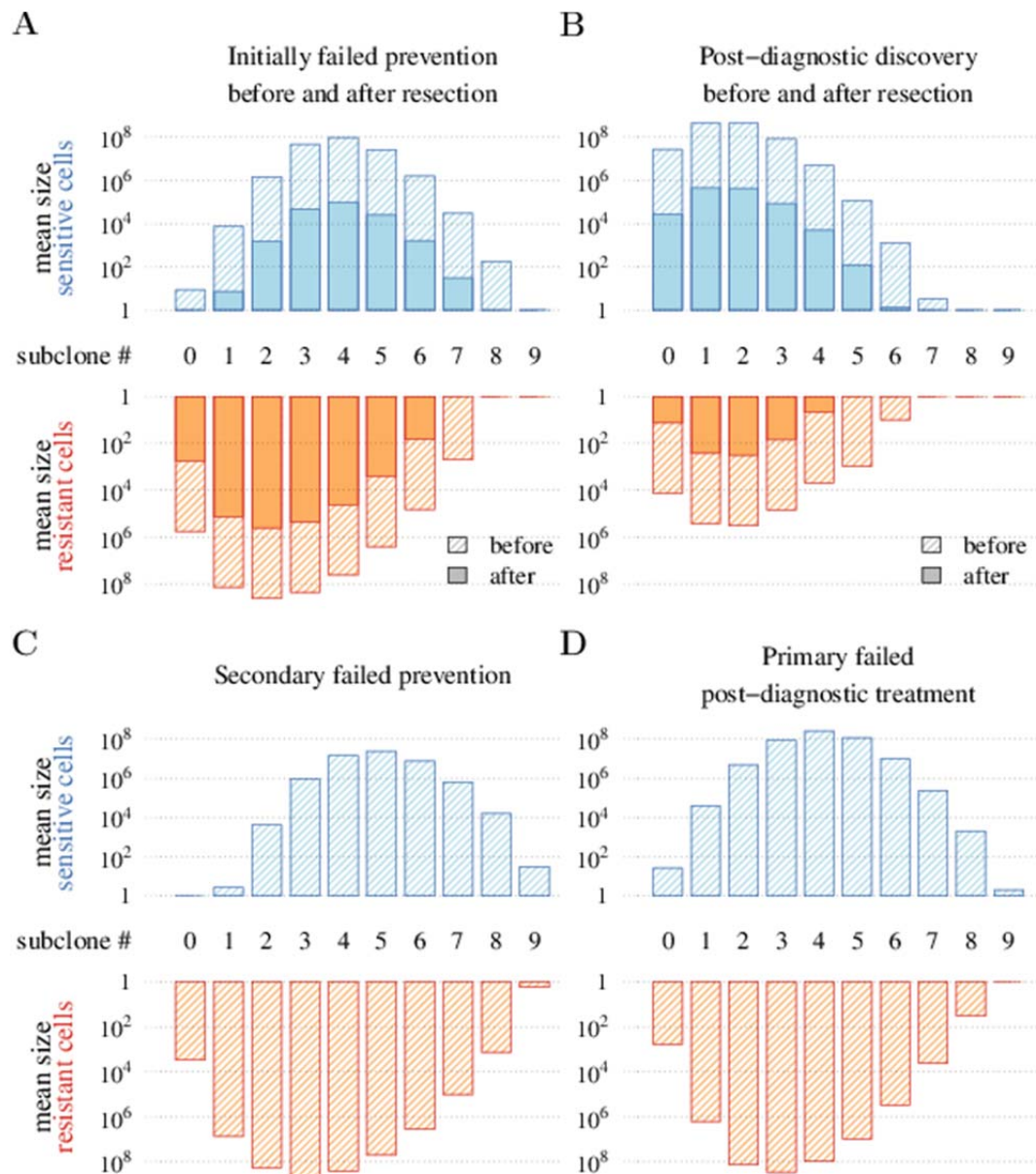


Figure 5 – figure supplement 2. Distribution of mean sizes of subclones (additional drivers). (A) Cases where a tumour is detected and resected following prevention. (B) Cases where a tumour is detected and resected with no prevention. (C) Cases of relapse following resection and secondary treatment to initially failed prevention. (D) Cases of relapse following resection and primary treatment in cases where there was no prevention. Hatched bars indicate cell numbers in the tumour, and solid bars numbers after resection and 10^6 residual or metastatic cells. Daily arresting level assumed to be 0.25%. Parameter values as in Table 1.

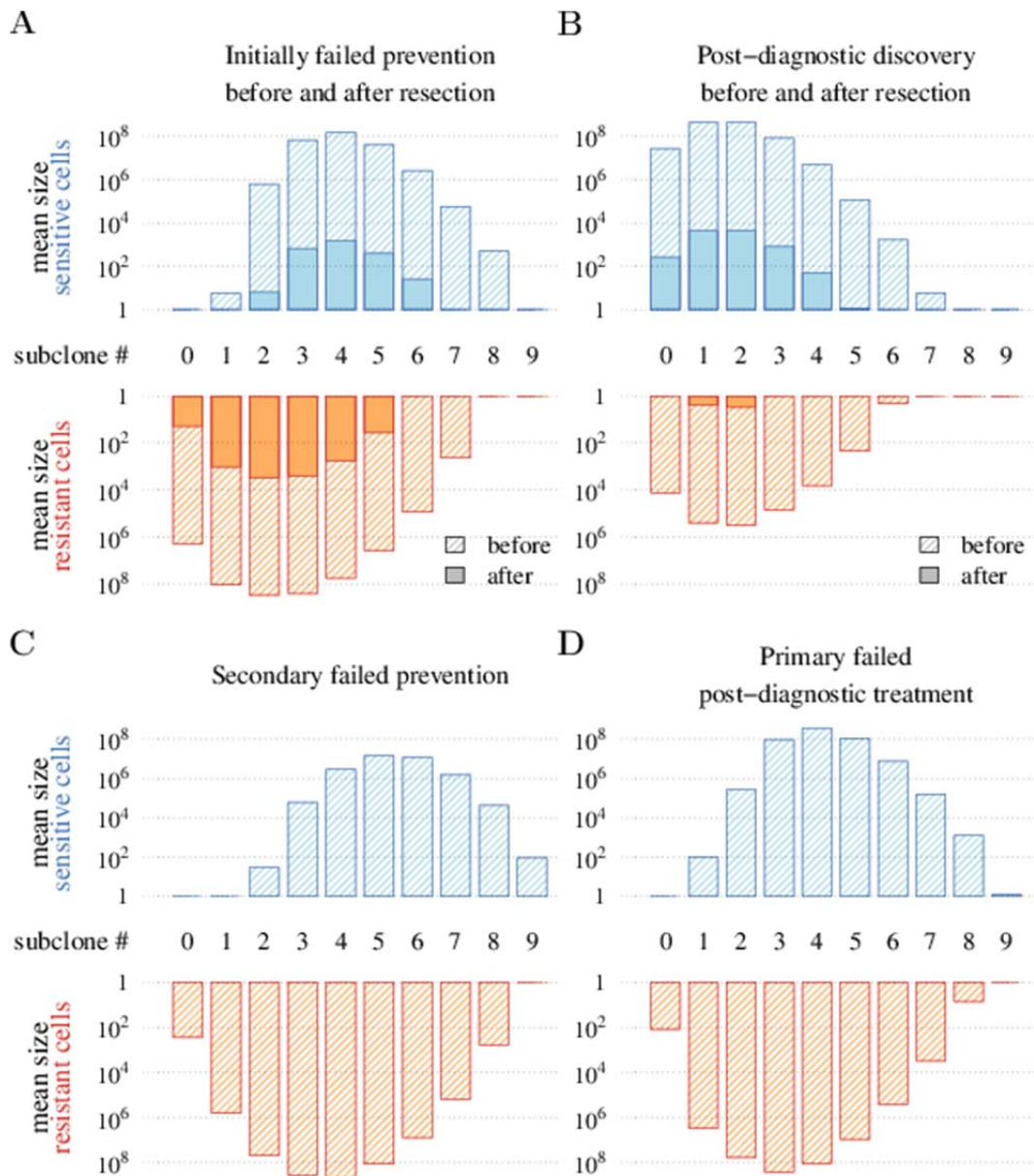


Figure 5 – figure supplement 3. Same as Figure 5 – figure supplement 2, except M_0 (initial population of preventatively treated cells and residual cell population number after resection) is 10^4 cancer cells.

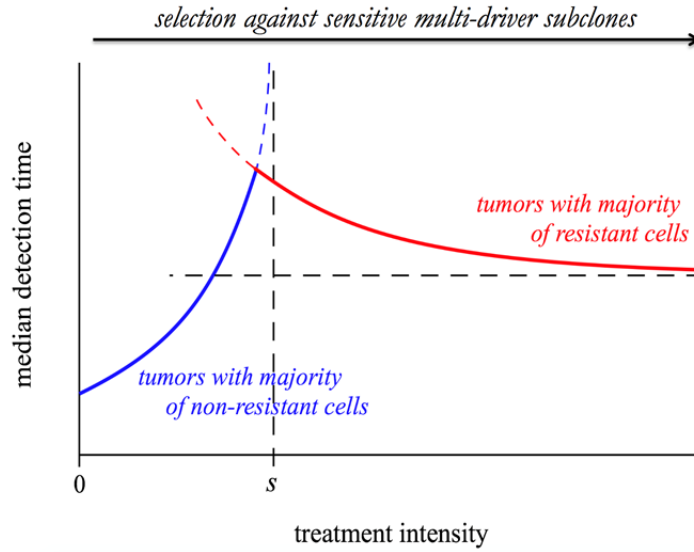


Figure 6. Schematic representation of the dependence of the median time for tumour detection on treatment intensity σ per cell-cycle. Increasing treatment intensity selects against subclones with increasing numbers of drivers, however it also selects for subclones with resistance mutations. The solid coloured line is subdivided into two parts: one where the detected tumours consist of mainly non-resistant cells (shown in blue), and the other mainly resistant cells (shown in red). The line approaches a horizontal asymptote for large treatment intensities, whereas if the resistant mutation were to be knocked out, the vertical asymptote at $\sigma = s$ would be approached instead. Both asymptotes are shown as dashed lines.

Supplementary videos

Please visit

Video 1: Contains Supplementary Videos 1-3

- <http://tiny.cc/AkhmHoch15SVideos123>

Treatment level affects both detection time and frequency of resistance. (A) The median (thick line) and 90% confidence intervals (shaded areas with dashed boundaries) for the distribution of detection times. (B) Arbitrary samples of the distribution of detection times and distribution of the mean number of accumulated drivers. The colour-code indicates the average level of resistance in detected tumours over 3 month intervals. Unless otherwise specified, parameters as in Table 1.

Video 2: Contains Supplementary Videos 4-5

- <http://tiny.cc/AkhmHoch15SVideos45>

Comparison of preventive (blue lines and shading) and post-diagnostic (red lines, hatched) interventions. (A) The median (thick line) and 90% confidence intervals (shaded areas with dashed boundaries) for the distribution of times to relapse for treatment failures. (B) and (C) Arbitrary samples of the distribution of detection times for preventive and post-diagnostic interventions, respectively. The colour-code indicates the mean number of accumulated drivers for a period of 1 year. The rectangle on the top of B and on the bottom of C shows the 5th and 95th percentiles, the blue circle indicates the median, and the red line is the mean. Parameters as in Table 1.

Appendix 1

A. Mean-field approach

We use the mean-field approach, see *e.g.* (30), which approximates the behaviour of a system consisting of many cells, so that the effects of stochasticity are averaged and an intermediate state is described by a set of ordinary differential equations.

Master equations

We write master equations to track the probability $P_{ij}(t)$ that a randomly chosen cell from a population of tumour cells is of type (i, j) at time t .

The temporal dynamics of probabilities $P_{ij}(t)$, $i = 0, 1, \dots, N$, where N is the maximal number of additionally acquired drivers and $j = 0, 1$, are described by

$$\frac{dP_{ij}(t)}{dt} = \mathbb{P}_{ij} + u\mathbb{P}_{ij}^{(u)} + v\mathbb{P}_{ij}^{(v)}.$$

Here, the right-hand side is a superposition of probabilistic in- and out-flows from different mutational states to the current one (i, j) . The function \mathbb{P}_{ij} describes the growth of subclone (i, j) and is proportional to the probability $P_{ij}(t)$, multiplied by the difference between fitness f_{ij} and its average value over the whole population $\bar{f}(t) = \sum_{i,j} f_{ij}P_{ij}(t)$. Functions $\mathbb{P}_{ij}^{(u)}$ and $\mathbb{P}_{ij}^{(v)}$ represent the probabilistic flows of mutations. For $\mathbb{P}_{ij}^{(u)}$, a driver is added from class $(i-1, j)$ to (i, j) in proportion to the probability $P_{i-1,j}(t)$, the probability of cell birth $b_{i-1,j}$, and the probability of a zero locus being chosen from N total loci consisting of $(N - (i-1))$ other zero loci. A similar approach is used to define the outflow term for the probability from class (i, j) to $(i+1, j)$. The second term $\mathbb{P}_{ij}^{(v)}$ is the probability of mutating to therapeutic resistance $(i, j = 0)$ to $(i, j = 1)$, and is proportional to $P_{i0}(t)$ and birth rate b_{i0} . Finally, all terms are summed, taking into account the initial conditions: $P_{00}(0) = 1 - \kappa$, $P_{01}(0) = \kappa$ and $P_{ij} = 0$ for any other i or j .

The above elements lead to the following system of ordinary differential equations (ODEs):

$$\begin{aligned} \frac{dP_{ij}(t)}{dt} = & \left(f_{ij} - \bar{f}(t) \right) P_{ij}(t) \\ & + u \left[\left(1 - \frac{i-1}{N} \right) \frac{1 + f_{i-1,j}}{2} P_{i-1,j}(t) - \left(1 - \frac{i}{N} \right) \frac{1 + f_{ij}}{2} P_{ij}(t) \right] \\ & - v(1-2j) \frac{1 + f_{i0}}{2} P_{i0}(t), \end{aligned} \quad (1)$$

892 where some probabilities $P_{ij}(t)$ could, theoretically, take on negative values, *e.g.* $P_{-1,j}(t)$, when
 893 $i = 0$, in which case, they are set to zero.

894 A simple transformation

$$p_{ij}(0) = P_{ij}(0), p_{ij}(t) = P_{ij}(t) \exp\left(\int_0^t \bar{f}(r) dr\right),$$

895 allows omitting the term $\bar{f}(t)$ from Eq. (1) and to linearize the latter with respect to the new
 896 “transformed” probabilities $p_{ij}(t)$. This gives

$$\begin{aligned} \frac{dp_{ij}(t)}{dt} = & f_{ij}p_{ij}(t) + u \left[\left(1 - \frac{i-1}{N}\right) \frac{1+f_{i-1,j}}{2} p_{i-1,j}(t) - \left(1 - \frac{i}{N}\right) \frac{1+f_{ij}}{2} p_{ij}(t) \right] \\ & + v \frac{1+f_{i0}}{2} (jp_{i,j-1}(t) + (j-1)p_{ij}(t)), \end{aligned} \quad (2)$$

897 where, for convenience, we write $(jp_{i,j-1}(t) + (j-1)p_{ij}(t))$ instead of $(1-2j)p_{i0}(t)$.

898 **Probability generating function approach**

899 With the master equations (2), we apply the probability generating function (p.g.f.) method
 900 (31,73) to transform the system of $(2N + 1)$ ODEs to a Hamilton-Jacobi (HJ) equation, that is, a
 901 first order partial differential equation.

902 We define the p.g.f. as the polynomial over all modified probabilities $p_{ij}(t)$ of the form

$$G(\xi, \eta, t) = \sum_{i=0}^N \sum_{j=0}^1 \xi^i \eta^j p_{ij}(t), \quad (3)$$

903 where ξ and η are variables that can be viewed as the momentum of an auxiliary Hamiltonian
 904 system governing the leading-order stochastic dynamics of the system (74). Notice that the
 905 function $G(\xi, \eta, t)$ is linear with respect to η .

906 Suppose that the function $G(\xi, \eta, t)$ is defined, one can then obtain all characteristics of the
 907 stochastic process such as the average tumour size $n(t)$ and the average frequency $n_{res}(t)/n(t)$
 908 of resistant cells within a tumour. The former quantity is

$$\frac{dn(t)}{dt} = n(t)\bar{f}(t).$$

909 Using the normalization condition for the probability: $\sum_{i,j} P_{ij}(t) = 1$, we obtain

$$G(\xi = 1, \eta = 1, t) = \exp\left(\int_0^t \bar{f}(r) dr\right),$$

910 and then

$$n(t) = M_0 \exp\left(\int_0^t \bar{f}(r) dr\right) = M_0 G(\xi = 1, \eta = 1, t), \quad (4)$$

911 where the initial tumour size $n(0) = M_0$ is sufficiently large. The frequency of resistant cells is
 912 defined as follows

$$\frac{n_{res}(t)}{n(t)} = \sum_{i=0}^N P_{i1}(t) = \sum_{i=0}^N p_{i1}(t) \exp\left(-\int_0^t \bar{f}(r) dr\right) = \frac{\partial G / \partial \eta}{G(\xi, \eta, t)} \Big|_{\xi=1, \eta=1}. \quad (5)$$

913 Initial conditions yield $p_{00}(0) = 1 - \kappa$, $p_{01}(0) = \kappa$ and $p_{ij}(0) = 0$ for any other i and j , so that
 914 $G(\xi, \eta, t = 0) = 1 - \kappa + \kappa\eta$.

915 To obtain the HJ equation related to the p.g.f. $G(\xi, \eta, t)$, we multiply (2) on $\xi^i \eta^j$ and sum up all
 916 equations for $i = 0, 1, \dots, N$ and $j = 0, 1$. After some algebra, we obtain

$$\begin{aligned} \frac{\partial G}{\partial t} = & \left[s \left(\xi \frac{\partial}{\partial \xi} + 1 \right) - \sigma \left(1 - \eta \frac{\partial}{\partial \eta} \right) - c\eta \frac{\partial}{\partial \eta} + \frac{u(\xi - 1)}{2} \left(1 - \frac{\xi}{N} \frac{\partial}{\partial \xi} \right) \right. \\ & \left. + \frac{v(\eta - 1)}{2} \left(1 - \eta \frac{\partial}{\partial \eta} \right) \right] G, \end{aligned} \quad (6)$$

917 where only terms of order greater than or equal to u , v are retained, meaning that terms composed
 918 of the products s , c and u , v are omitted.

919 Equation (6) is solved by the method of characteristics such that the HJ equation is transformed
 920 into a system of ordinary differential equations (*i.e.*, the system of characteristics, see *e.g.* (75)).

921 **Time-varied treatment schedule**

922 We find the characteristics for the variables ξ and η using (6):

$$\frac{d\xi(t)}{dt} = -s\xi(t) + \frac{u\xi(t)(\xi(t) - 1)}{2N}, \quad \frac{d\eta(t)}{dt} = (c - \sigma(t))\eta(t) + \frac{v\eta(t)(\eta(t) - 1)}{2}, \quad (7)$$

923 where $\sigma(t)$ is a given function of time.

924 The p.g.f. $G(\xi, \eta, t)$ changes along the characteristic (7) according to the following ODE

$$\frac{dG(t)}{dt} = \left(s - \sigma + \frac{u(\xi(t) - 1)}{2} + \frac{v(\eta(t) - 1)}{2} \right) G(t), \quad (8)$$

925 which is straightforward to integrate. Indeed, if we use (7), this yields: $d \ln G = (s(N + 1) -$
 926 $c)dt + Nd \ln \xi + d \ln \eta$. Thus,

$$G(\xi, \eta, t) \exp[-(s(N + 1) - c)t - N \ln \xi - \ln \eta] = \text{const.} \quad (9)$$

Recall that the quantity on the left hand side remains constant only along the characteristic curve (7).

To obtain $G(\xi = 1, \eta = 1, t)$, we need to solve (7) subject to $\xi(t) = \eta(t) = 1$ and find $\xi(0)$ and $\eta(0)$. Then, given the initial condition $G(\xi(0), \eta(0), 0) = 1 - \kappa + \kappa\eta(0)$, κ is a level of resistance within a tumour ($\kappa \in [0, 1]$), we can define $G(\xi, \eta, t)$ using (9).

Finally, we use (4) to derive the dynamics of $n(t)$. To obtain the mean frequency of resistant cells within a tumour, we first write $\partial G / \partial \eta$, using (9) with the right hand side implicitly dependent on η and then substitute it into (5). (Note that time t is measured in cell cycles, which are assumed to be of 4 days on average. To derive all necessary equations with respect to the actual time, we need to divide t by the length of the cell-cycle T and substitute it in the equations.)

Constant treatment

We study the case for constant σ . Notice that this includes the case of no treatment ($\sigma = 0$).

First, we find the characteristics for the variables ξ and η . Namely, solution of (7) gives

$$\begin{aligned} \xi(0) &= \frac{s + u/(2N)}{\left(\frac{s + u/(2N)}{\xi(t)} - \frac{u}{2N}\right) e^{-(s+u/(2N))t} + \frac{u}{2N}}, \eta(0) \\ &= \frac{\sigma - c + v/2}{\left(\frac{\sigma - c + v/2}{\eta(t)} - \frac{v}{2}\right) e^{-(\sigma-c+v/2)t} + \frac{v}{2}} \end{aligned} \quad (10)$$

The subsequent substitution of (10) into (8) leads to

$$\begin{aligned} G(\xi, \eta, t) &= G(\xi(0), \eta(0), 0) \exp \left[\left(s - \sigma - \frac{u + v}{2} \right) t \right. \\ &\quad \left. + N \ln \left(1 + \frac{\xi u}{2N} \frac{e^{(s+u/(2N))t} - 1}{s + u/(2N)} \right) + \ln \left(1 + \frac{\eta v}{2} \frac{e^{(\sigma-c+v/2)t} - 1}{\sigma - c + v/2} \right) \right]. \end{aligned}$$

Taking into account $u, v \ll s, c$ and assuming $v \ll \sigma - c$, we simplify further and write its approximate form

$$\begin{aligned} G(\xi, \eta, t) &\cong \left(1 - \kappa + \frac{\kappa \eta e^{(\sigma-c)t}}{1 + \frac{\eta v}{2} \frac{e^{(\sigma-c)t} - 1}{\sigma - c}} \right) \\ &\exp \left[(s - \sigma)t + N \ln \left(1 + \frac{\xi u}{2N} \frac{e^{st} - 1}{s} \right) + \ln \left(1 + \frac{\eta v}{2} \frac{e^{(\sigma-c)t} - 1}{\sigma - c} \right) \right], \end{aligned}$$

which can be also written in the form

$$G(\xi, \eta, t) \cong \left((1 - \kappa) \left(1 + \frac{\eta v e^{(\sigma-c)t} - 1}{2(\sigma - c)} \right) + \kappa \eta e^{(\sigma-c)t} \right) \exp \left[(s - \sigma)t + N \ln \left(1 + \frac{\xi u e^{st} - 1}{2N s} \right) \right]. \quad (11)$$

946 As expected (11) is linear with respect to η .

947 Thus, we derive an analytical expression for the dynamics $n(t)$. Namely, we use (4), (11) and
948 substitute $\xi = \eta = 1$, to obtain

$$n(t) = M_0 \left((1 - \kappa) \left(1 + \frac{v e^{(\sigma-c)t} - 1}{2(\sigma - c)} \right) + \kappa e^{(\sigma-c)t} \right) \exp \left[(s - \sigma)t + N \ln \left(1 + \frac{u e^{st} - 1}{2N s} \right) \right]. \quad (12)$$

949 Equation (12) is simplified for two limiting cases. In the early stages of tumour growth, the value
950 $n(t)$ changes according to a hyper-exponential law

$$n(t) \cong M_0 \left((1 - \kappa) \left(1 + \frac{v e^{(\sigma-c)t} - 1}{2(\sigma - c)} \right) + \kappa e^{(\sigma-c)t} \right) \exp \left((s - \sigma)t + \frac{u e^{st} - 1}{2 s} \right),$$

951 while at later stages the most aggressive subclone persists, being sensitive if $\sigma < c$ ($n(t) \propto$
952 $e^{s(N+1)t}$) and resistant otherwise ($n(t) \propto e^{(s(N+1)-c)t}$).

953 To compute the frequency of resistant cells within a tumour (5), we derive $\partial G / \partial \eta$ using (11):

$$\frac{\partial G}{\partial \eta} = \left((1 - \kappa) \frac{v e^{(\sigma-c)t} - 1}{2(\sigma - c)} + \kappa e^{(\sigma-c)t} \right) \exp \left[(s - \sigma)t + N \ln \left(1 + \frac{\xi u e^{st} - 1}{2N s} \right) \right].$$

954 so that

$$\frac{n_{res}(t)}{n(t)} = \frac{(1 - \kappa) \frac{v e^{(\sigma-c)t} - 1}{2(\sigma - c)} + \kappa e^{(\sigma-c)t}}{(1 - \kappa) \left(1 + \frac{v e^{(\sigma-c)t} - 1}{2(\sigma - c)} \right) + \kappa e^{(\sigma-c)t}}.$$

955 Appendix 1 – figure 1 show the excellent correspondence between numerical experiments and
956 analytical results for σ on the order of s . Appendix 1 – figure 2 provides additional details on
957 distribution of tumour sizes depending on the applied treatment intensity (points B and C).

958 **Distribution of subclones within an exponentially growing tumour**

959 The p.g.f. $G(\xi, \eta, t)$ is used to derive expressions for all $P_{ij}(t)$, which are the probabilities of
 960 selecting a cell of type (i, j) from a tumour at time moment t . Namely, we need to differentiate
 961 the p.g.f. with respect to ξ and η , so that

$$P_{ij}(t) = \frac{1}{i! G(\xi = 1, \eta = 1, t)} \frac{\partial^{i+j} G(\xi = 0, \eta = 0, t)}{\partial \xi^i \partial \eta^j},$$

962 where $i = 0, 1, \dots$ and $j = 0, 1$. Thus, we write

$$P_{00}(t) = \frac{G(0,0,t)}{G(1,1,t)} = \frac{1 - \kappa}{(1 - \kappa) \left(1 + \frac{v}{2} \frac{e^{(\sigma-c)t} - 1}{\sigma - c}\right) + \kappa e^{(\sigma-c)t}} \left(1 + \frac{u}{2N} \frac{e^{st} - 1}{s}\right)^{-N},$$

$$P_{01}(t) = \frac{\partial G(0,0,t)/\partial \eta}{G(1,1,t)} = \frac{(1 - \kappa) \frac{v}{2} \frac{e^{(\sigma-c)t} - 1}{\sigma - c} + \kappa e^{(\sigma-c)t}}{(1 - \kappa) \left(1 + \frac{v}{2} \frac{e^{(\sigma-c)t} - 1}{\sigma - c}\right) + \kappa e^{(\sigma-c)t}} \left(1 + \frac{u}{2N} \frac{e^{st} - 1}{s}\right)^{-N},$$

963 then

$$P_{10}(t) = \frac{\partial G(0,0,t)/\partial \xi}{G(1,1,t)} = \frac{1 - \kappa}{(1 - \kappa) \left(1 + \frac{v}{2} \frac{e^{(\sigma-c)t} - 1}{\sigma - c}\right) + \kappa e^{(\sigma-c)t}} \frac{u}{2} \frac{e^{st} - 1}{s} \left(1 + \frac{u}{2N} \frac{e^{st} - 1}{s}\right)^{-N},$$

$$P_{11}(t) = \frac{1}{G(1,1,t)} \frac{\partial^2 G(0,0,t)}{\partial \xi \partial \eta} = \frac{(1 - \kappa) \frac{v}{2} \frac{e^{(\sigma-c)t} - 1}{\sigma - c} + \kappa e^{(\sigma-c)t}}{(1 - \kappa) \left(1 + \frac{v}{2} \frac{e^{(\sigma-c)t} - 1}{\sigma - c}\right) + \kappa e^{(\sigma-c)t}} \frac{u}{2} \frac{e^{st} - 1}{s} \left(1 + \frac{u}{2N} \frac{e^{st} - 1}{s}\right)^{-N},$$

964 The general formula is written as follows

$$P_{i0}(t) = \frac{1}{i! G(1,1,t)} \frac{\partial^i G(0,0,t)}{\partial \xi^i} = \frac{1 - \kappa}{(1 - \kappa) \left(1 + \frac{v}{2} \frac{e^{(\sigma-c)t} - 1}{\sigma - c}\right) + \kappa e^{(\sigma-c)t}} P_{i*}(t),$$

$$P_{i1}(t) = \frac{1}{i! G(1,1,t)} \frac{\partial^{i+1} G(0,0,t)}{\partial \xi^i \partial \eta} = \frac{(1 - \kappa) \frac{v}{2} \frac{e^{(\sigma-c)t} - 1}{\sigma - c} + \kappa e^{(\sigma-c)t}}{(1 - \kappa) \left(1 + \frac{v}{2} \frac{e^{(\sigma-c)t} - 1}{\sigma - c}\right) + \kappa e^{(\sigma-c)t}} P_{i*}(t),$$

965 where $i = 0, 1, \dots, N$ and the function

$$P_{i*}(t) = \binom{N}{i} \left(\frac{u}{2N} \frac{e^{st} - 1}{s}\right)^i \left(1 + \frac{u}{2N} \frac{e^{st} - 1}{s}\right)^{-N}$$

966 defines the probability to pick a cell with i drivers independently of resistant status, $P_{i*}(t) \triangleq$
 967 $P_{i0}(t) + P_{i1}(t)$, where $\binom{N}{i}$ denotes a binomial coefficient, equal $\frac{N!}{i!(N-i)!}$.

968 The distribution $P_{i*}(t)$ for a particular case of $N = 6$ is shown in Appendix 1 – figure 3.

969 We now derive the mean time period when a given subclone with i additionally accumulated
 970 drivers dominates within a tumour.

971 Defining the time moments $t = t_i$ for which $P_{i-1,*}(t_i) = P_{i*}(t_i)$ ($i = 0, 1, 2, \dots, N$) gives

$$t_i = \frac{1}{s} \ln \left(1 + \frac{2sNi}{u(N-i+1)} \right) \approx \frac{1}{s} \ln \frac{2sNi}{u(N-i+1)},$$

972 where we assume $u \ll s$.

973 The time period when the subclone with i drivers prevails in a cell population is defined by the
 974 following expression

$$\begin{aligned} \Delta t_i = t_{i+1} - t_i &= \frac{1}{s} \left[\ln \left(1 + \frac{2sN(i+1)}{u(N-i)} \right) - \ln \left(1 + \frac{2sNi}{u(N-i+1)} \right) \right] \\ &\approx \frac{1}{s} \ln \frac{(N-i+1)(i+1)}{(N-i)i}, \end{aligned}$$

975 where $i \neq 0$. For $i = 0$, we have

$$\Delta t_0 = \frac{1}{s} \ln \left(1 + \frac{2s}{u} \right) \approx \frac{1}{s} \ln \frac{2s}{u}.$$

976 The latter formula has been previously reported (see eqn. S7 in reference (27)).

977 **B. Varying mutation rate and initial tumour size**

978 To understand better how the inflection points arise around $\sigma = qs$ ($q = 1, 2, 3, \dots$), we first
 979 consider a much simpler case than the main text. Suppose that no additional driver mutation is
 980 acquired during tumorigenesis, $u = 0$. Any treatment regime of constant intensity lower than the
 981 selective advantage ($\sigma < s$) only slows tumour growth. In such cases the median detection time
 982 increases with σ (see Figure 6). Assuming that resistance is not obtained, the median time to
 983 detection approaches a vertical asymptote at $\sigma = s$, whereas the tumour is always eradicated for
 984 $\sigma > s$. If $v > 0$, then the tumour relapses following the appearance of the resistant mutation, and
 985 the median detection time approaches the horizontal asymptote for $\sigma \gg s$. Thus, the final result
 986 for the median detection time will be a line, consisting of two branches, shown in blue and red in
 987 Figure 6, intersecting at the point near $\sigma = s$.

988 In the general case ($u > 0, v > 0$), the median follows from the different elements cited above,
 989 consisting of several possible branches (e.g., Figure 2 – figure supplement 1B) or none, where the

latter case depends on the relation between the mutation rate u and the initial cell number M_0 (e.g., for $M_0 = 10^7$ in Figure 2 – figure supplement 1D).

Appendix 1 – figure 4 shows an example. Subfigure A demonstrates a case when u is varied and M_0 remains fixed. We identify the key parameter for appearance of the inflection points as M_0u . It defines the emergence probability of the next subclone with one additional driver. Hence, the inflection points are more apparent for smaller values of M_0u and vanish for larger values of M_0u . This same tendency can be seen in Figure 2 – figure supplement 1C, where M_0 is varied and u is fixed. Subfigures B, C and D provide more details on the interplay between the relation of M_0u and the manifestation of the inflection points.

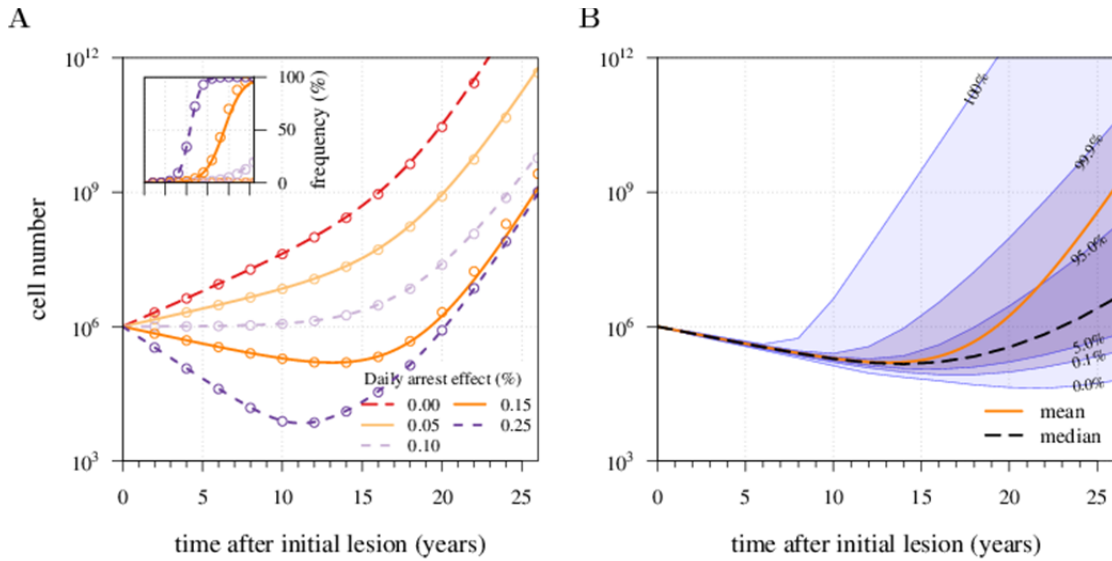
C. A simple form of drug addiction for resistant cell-lines

To explore the possible effects of drug addiction on tumour growth, we propose a simple modification of the fitness function. Suppose the cost of resistance C , is given by the relation

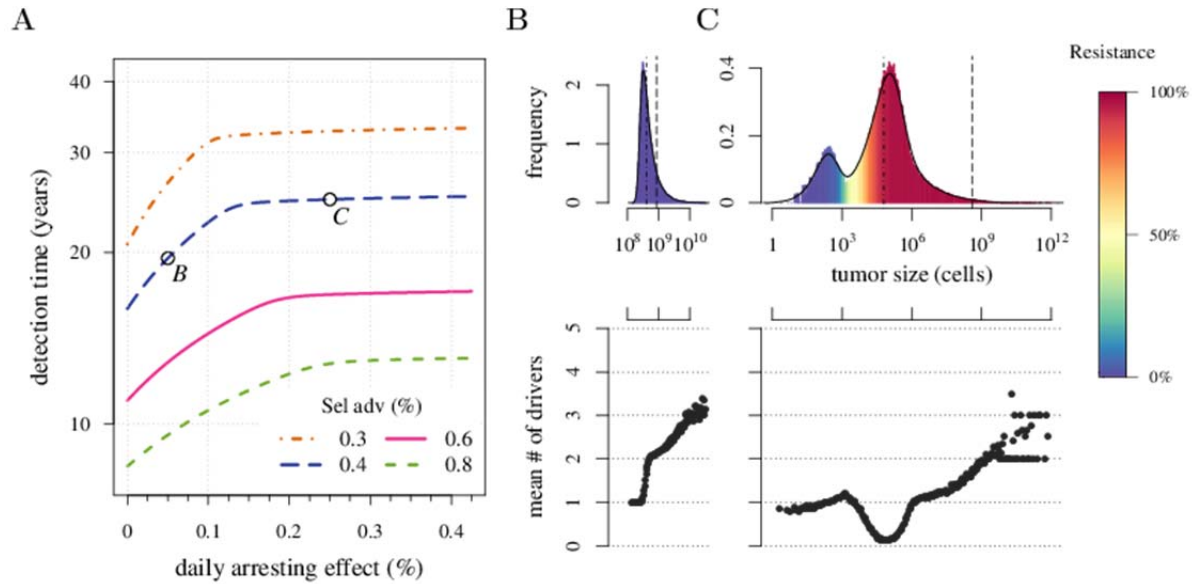
$$C = c \left(1 - \frac{2\sigma}{s} \right).$$

It equals c as before when no treatment is applied ($\sigma = 0$), while drug addiction increases with larger σ . The cost equals zero at $\sigma = 2s$ and becomes negative for $\sigma > 2s$, implying that further drug administration has a beneficial effect on proliferation of resistant cells. Fischer, Vásquez-García and Mustonen (40) argue that under drug addiction, a metronome treatment strategy is more beneficial than a constantly applied treatment. The metronome strategy imposes a simple rule: treatment is only applied when the number of non-resistant cells exceeds the number of resistant cells.

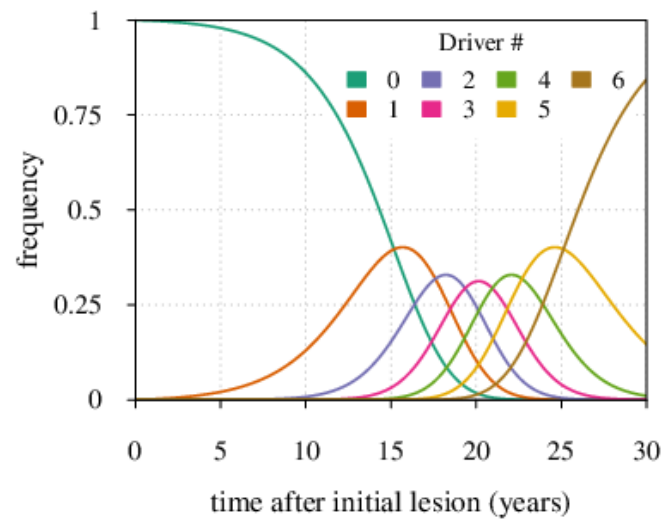
We compare the originally studied model, where the resistant cells exhibit no drug addiction, with a modified case of the drug addiction of resistant cells. In the latter, we consider two different treatment regimes: a constantly administrated drug application and metronome therapy. As an example, Appendix 1 – figure 5 shows, accounting for drug addiction worsens treatment outcomes with 5% vs. 31% eradicated tumours at daily arresting effect equal 0.25% ($\sigma = 1.0\%$) for presence vs. absence of drug addiction, respectively. Moreover, metronome therapy results in a better outcome than a constantly administrated chemotherapy. For example, the former adds 6.6 additional years to the median detection time at $\sigma = 1.0\%$, compared to the constant treatment with drug addiction, but loses 11.1 years, compared to the previous case of a constant treatment without drug addiction.



Appendix 1 – figure 1. Mean field dynamics concord with numerical simulations. (A) Effect of treatment level and observation time on mean tumour size. (**Inset**) Mean frequency of resistant cells within tumours corresponding to three of the cases in A. Lines are analytically computed mean-field trajectories, while dots are numerical simulations (see Appendix 1 for details). (B) Dynamics of mean and median tumour size, and percentiles around the median (shaded areas), assuming a fixed constant treatment of $\sigma = 0.6\%$ (daily arresting effect: 0.15%). Treatments start at $t = 0$, and the maximal number of additionally accumulated drivers is 3. See Table 1 for other parameter values.



Appendix 1 – figure 2. Trade-off between growth and resistance under different treatment regimes. (A) Analytically-derived times for a tumour to reach 10^9 cells (see equation (12)). (B) and (C) Sample distributions in relative frequencies, adjusted for bins over periods of 0.5 in logarithmic scale for corresponding points B and C, shown in plot A. Dashed black line is the mean and the dashed-and-dotted line is the median. The bottom panel shows the mean number of additionally accumulated drivers for all detected tumours over the same intervals of 3 months. The colour-code indicates the level of resistance in detected tumours over these intervals. Maximal number of additionally accumulated drivers is 5. Parameters otherwise as in Table 1.

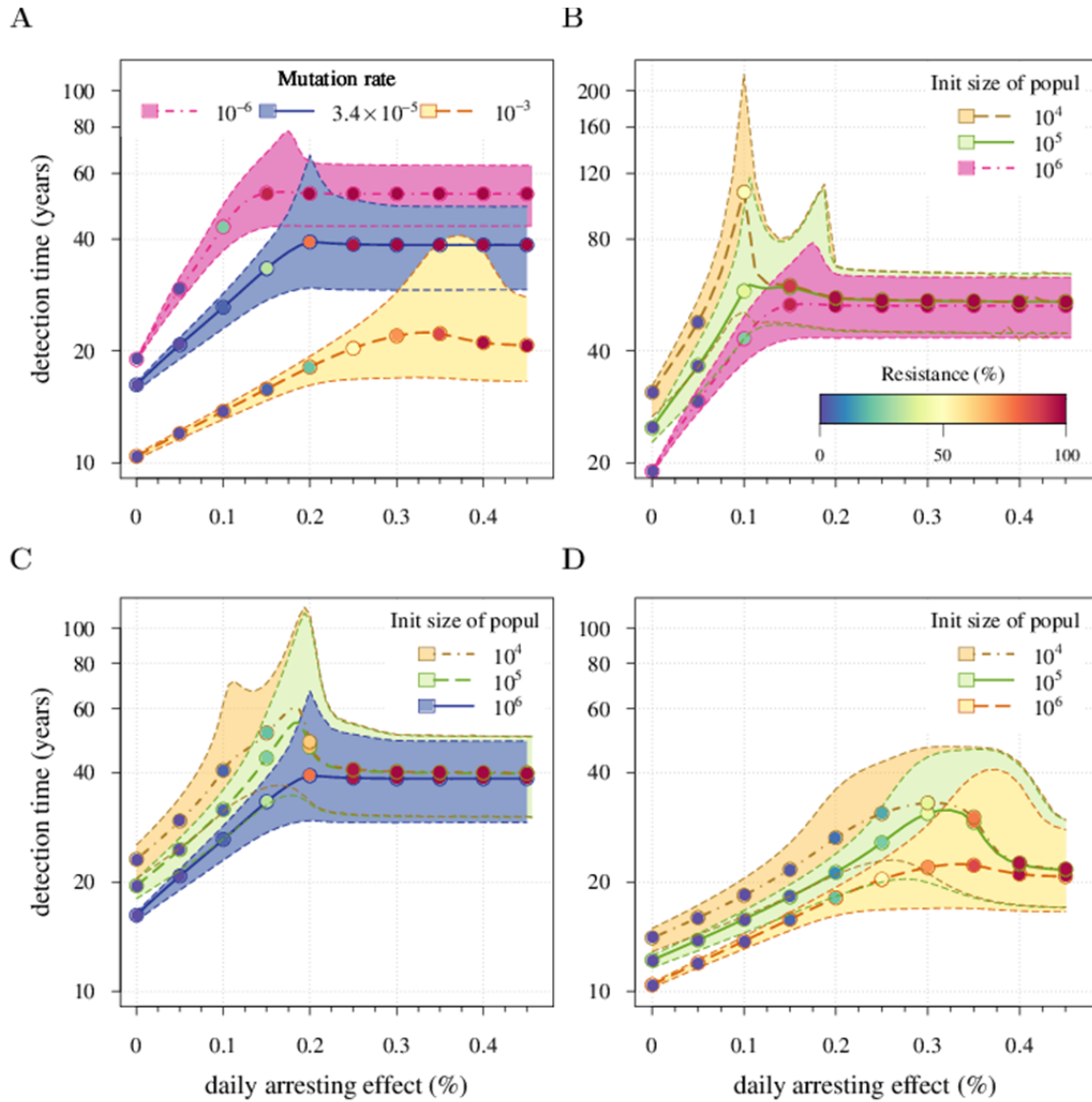


1037

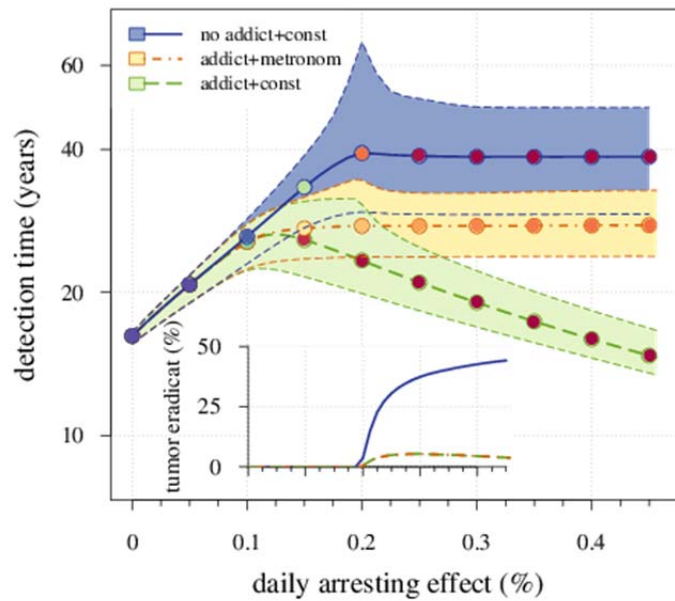
1038

1039

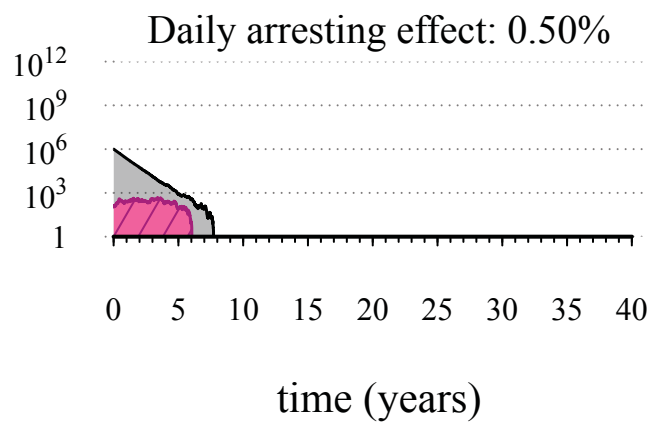
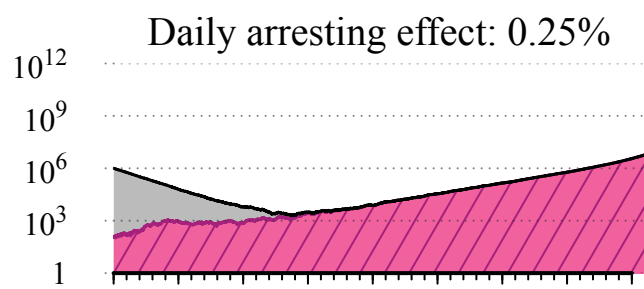
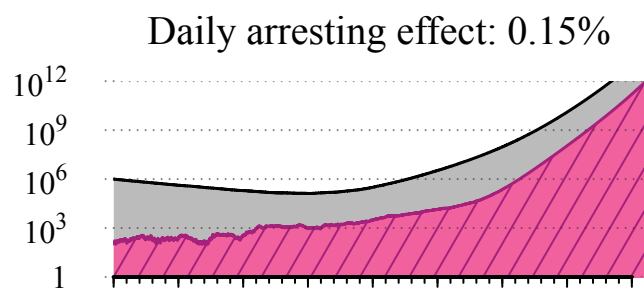
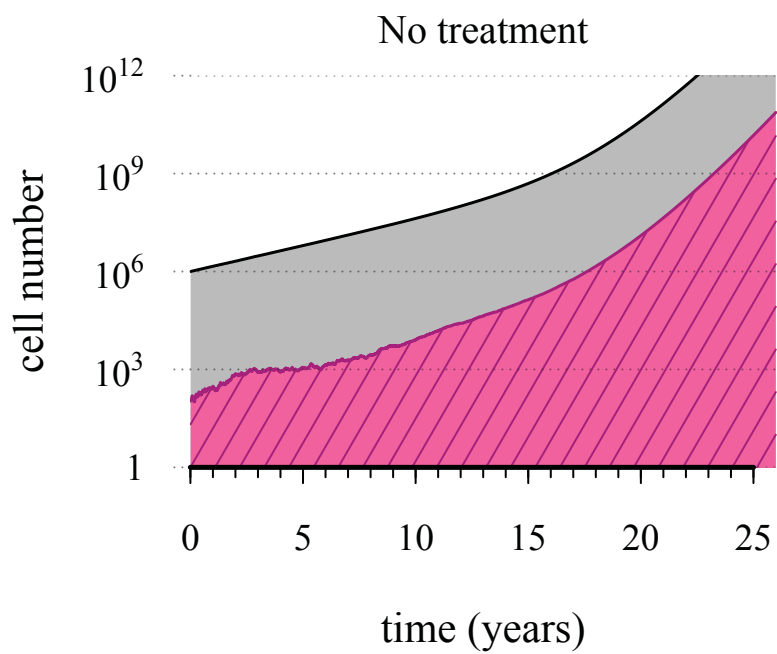
Appendix 1 – figure 3. Maximal tumour heterogeneity in terms of driver subclones occurs at intermediate times after initial lesion.



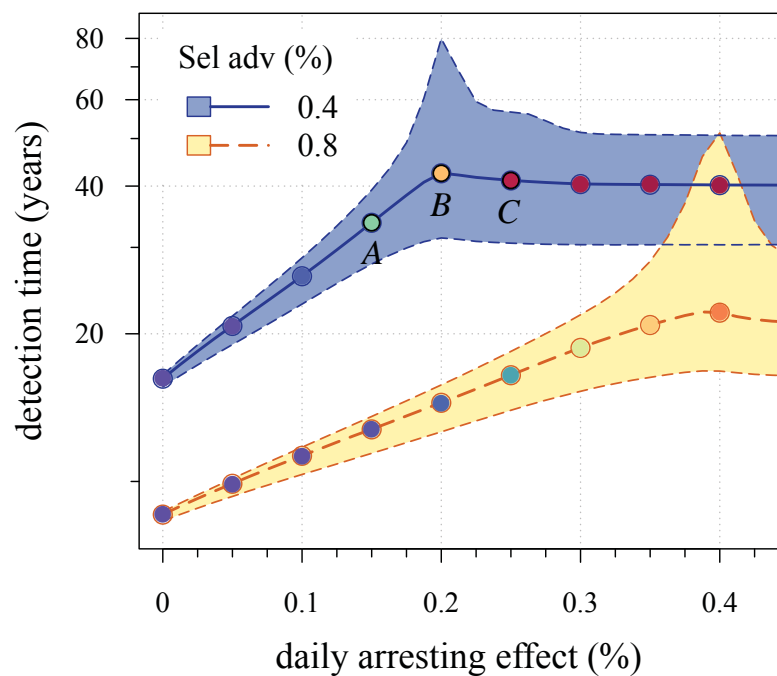
Appendix 1 – figure 4. Sensitivity analysis of (A) the mutation rate to acquire drivers and (B-D) initial tumour size. Thick lines indicate the median, and shaded areas with dashed boundaries the 90% confidence intervals of detection times. (A) Initial tumour size is fixed at 10⁶ cells and mutation rate is varied. (B-D) Initial tumour size is varied and mutation rate is fixed at (B) 10⁻⁶, (C) 3.4 × 10⁻⁵, (D) or 10⁻³. The colour code for points indicates the average level of resistance within tumours (see the inset in B). Parameter values are as in Table 1 except those being varied.



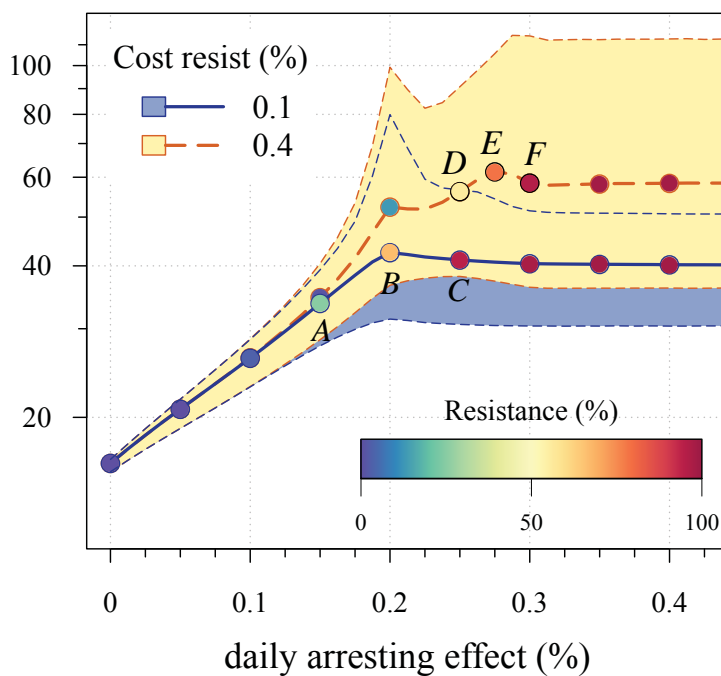
Appendix 1 – figure 5. Comparing a previously studied case (shown in blue in Figure 2) with the case where resistant cells may become addicted to the drug. The latter is illustrated by two treatment regimes: metronome strategy (shown in yellow) and constantly administrated drug (shown in green). The plot shows the median and 90% confidence intervals (shaded areas) of detection times. The inset presents the fraction of cases when the tumour goes extinct after the initial lesion of 10^6 cells. Parameters as in Table 1.



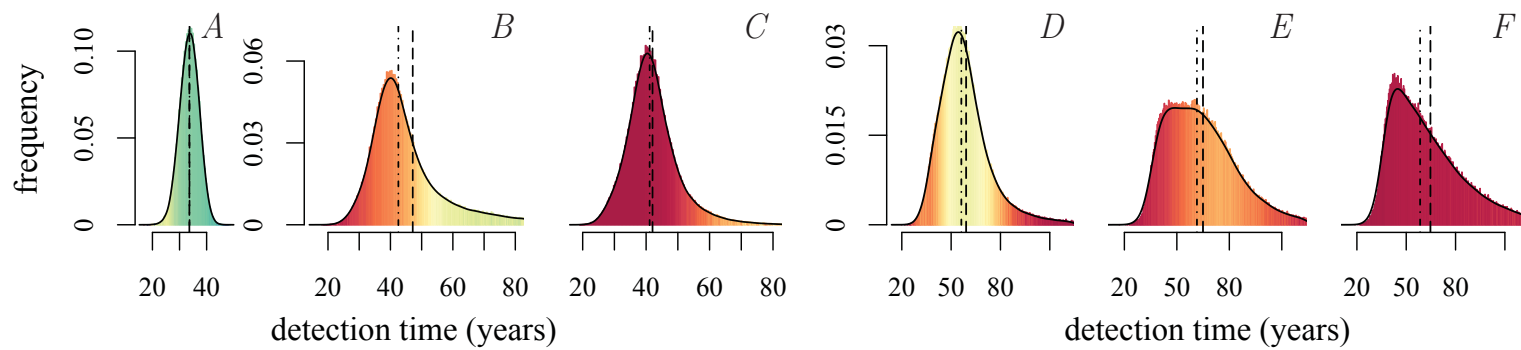
A



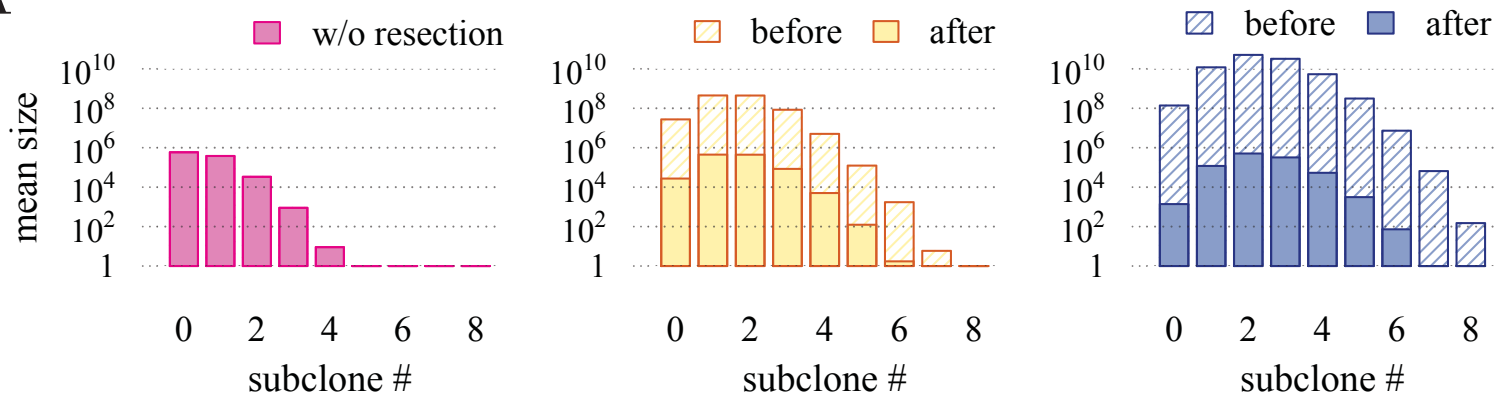
B



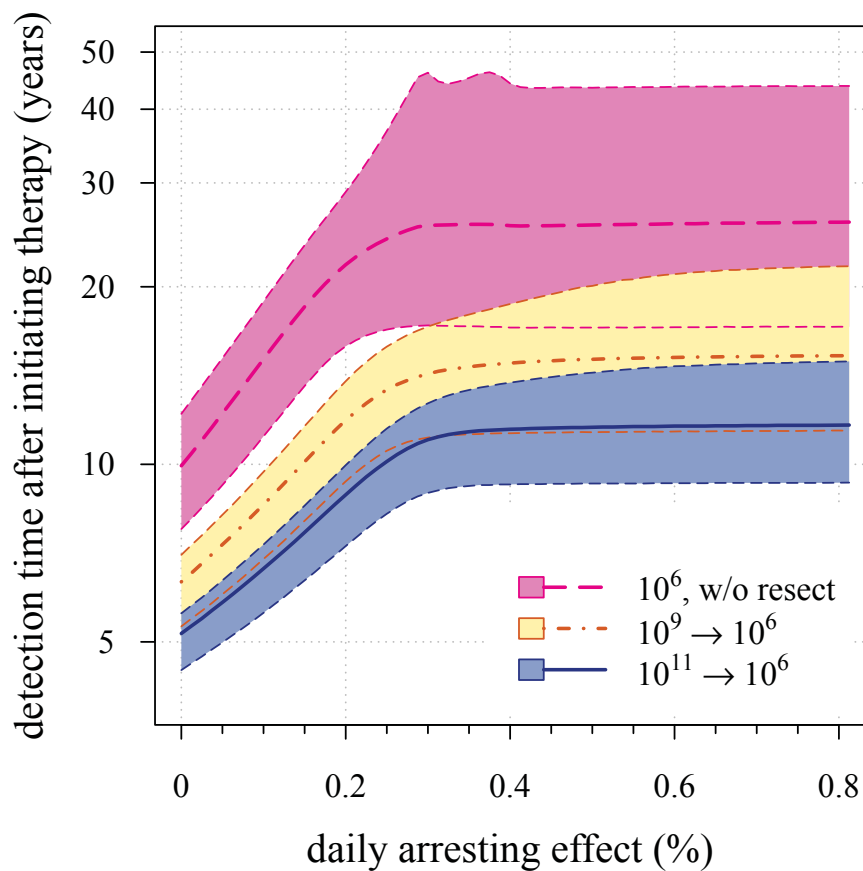
C



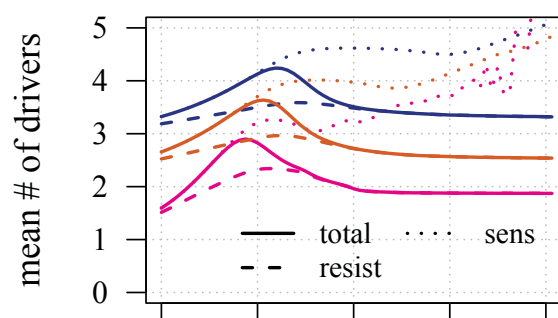
A



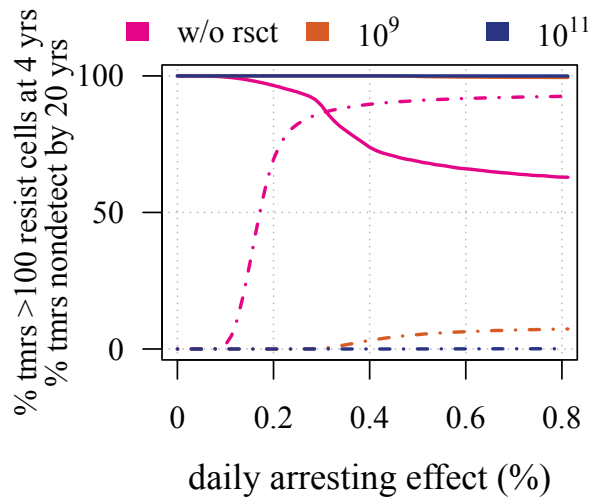
B



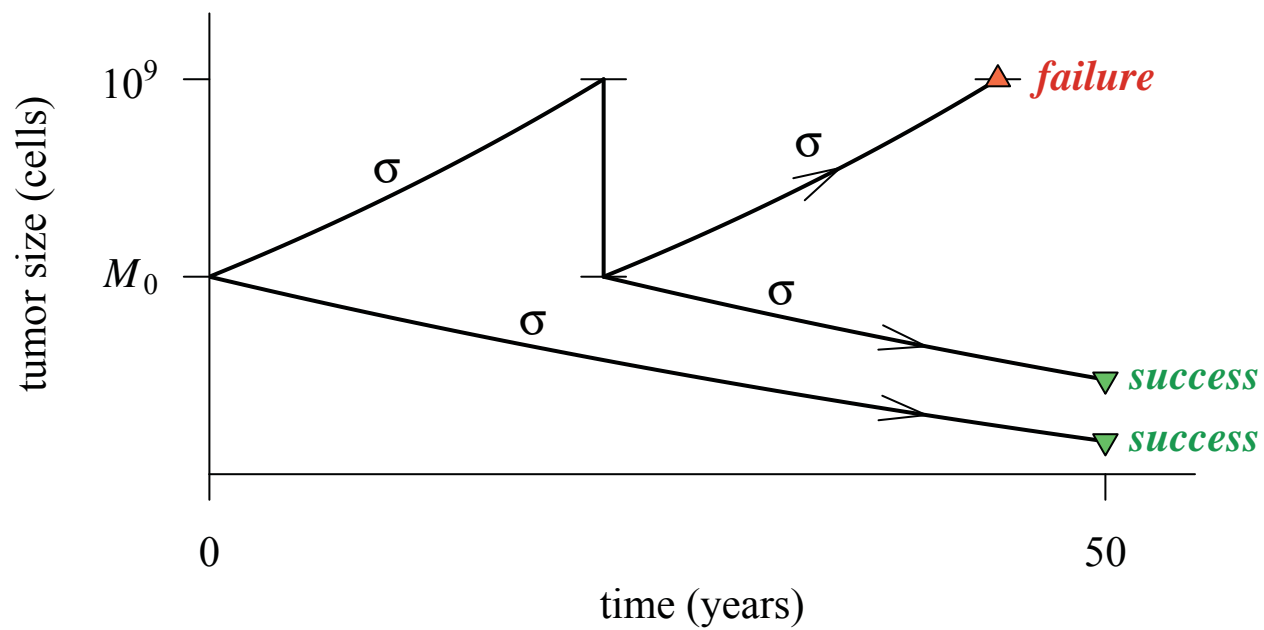
C



D



Prevention



Resection and treatment

